RESPONSE TO THE REFEREES

Dear editor,

Enclosed herewith please find the revision of the manuscript now entitled: “3D Reconstruction of Ocean Velocity from HFR and ADCP: a model-based assessment study”.

We sincerely acknowledge the reviewers for their careful review and their remarks. After analyzing their comments, we realized that neither the main idea nor the approach used to carry out our investigation were clear in the manuscript.

Therefore, major changes have been addressed throughout all the manuscript to correct these aspects and improve the readability of the paper.

Below are the reviewers’ comments, our detailed responses and the description of the modifications made in the manuscript. The attached new version of the paper explicitly shows all revisions in red.

We hope that, after the careful revision we have made by incorporating all reviewers' comments and sharpening the manuscript, our paper fulfils now the quality requirements of Ocean Science.

We are look forward to hearing from you at your earliest convenience.

Best regards,

Ivan Manso

Note that all the locations of the changes mentioned herein after correspond to the locations in the “clean” manuscript, not the marked-up version.

Anonymous Referee #1

Referee’s Comments

Review of “Three-Dimensional Reconstruction of Ocean Circulation from Coastal Marine Observations: Challenges and Methods”

Line 7, should technology be capitalized?

Line 16, should it read multiplatform or multisensory

Change to “aiming for the continuous”

Line 17, change from “is today” to “are”

Line 18, change to “resolution, but are limited to the”

The authors should make it more clear that the the ADCP and HFR data they are discussing were derived from model output. On the first read of the manuscript, I thought that data was from sensors deployed in the ocean.

Page 2

Line 27, change to “combining simulated information from ”

Line 30, change to “performance”

Page 3

Line 17, change to “with surface temperatures over”

Page 4

Line 1, remove Moreover

Page 5

Line 3, replace Summarizing with In summary,

Line 11, change to “surface current fields along the Mid Atlantic”

Page 6

Line 19, can the authors be more specific on what is meant by the observations and the reference fields

Page 7

What data source was used for the correlation scale tests, IBI, GLORYS-HR or GLORYS-LR?

Page 9

Figs 10-11 are mentioned before Figs 6-9, can this be changed

Page 12

Line 6, change to “the combination of synthetic data that mimics sensors from a

multiplatform observing system to reconstruct"

Author's comments

Dear reviewer,
First, thank you for your careful review of our manuscript and your remarks. They have been really helpful to improve the manuscript and we have addressed them into the text, as explained in the point by point responses further down. Thank you for your specific comments on the paper structure as well, since they helped to realize that the explanation of the approach that we used was not clear enough. We hope that thanks to your suggestions we have managed to improve the manuscript, and that it suits now the standards of Ocean Science.
Best regards,
Ivan Manso

AR = Author's response

AC = Author's changes in the manuscript

AC= After considering the comments of the two anonymous referees, major changes have been made in the manuscript. First, we have better defined the context of this work using, among others, the references proposed by referee#2 in order to get a more complete introduction with regard to studies for the expansion of HFR data to subsurface levels. We have also changed the Sect. 3.1 into Sect. 3 separating it from the main results (now in Sect. 4), thus leaving its own section to the description of the simulated 'true' ocean. We have also clarified the main aim, approach and conclusions of our work, with changes in several parts of the manuscript which are detailed in the following point by point responses.

Comments are enumerated

1- *Page 1, line 7: should technology be capitalized?*

   AR: Done.

   AC: in page 1 line 8

2- *Page 1, line 16: should it read multiplatform or multisensory. Change to "aiming for the continuous".*

   AR: Both terms could be used, but "multiplatform" is the term that better fits to the main focus of this paper, based on a model-based scenario where different platforms and sensors are measuring the same parameters and where different platforms are combined.

   AC: *"aiming for the continuous"* corrected in the manuscript in page 1 lines 16-17.

3- *Page 1, line 17: change from "is today" to "are".*

AR: We have maintained “is” because it refers to the percentage, thus “is today” was changed by “is”.

AC: “is today” was changed by “is” in page 1 line 17.

4- *Page 1, line 18: change to “resolution, but are limited to the”.*

AR: We have rephrased the entire sentence and we have removed that part.

AC: rephased sentence in page 1 lines 17-18.

5- *The authors should make it more clear that the the ADCP and HFR data they are discussing were derived from model output. On the first read of the manuscript, I thought that data was from sensors deployed in the ocean.*

AR: The reviewer is right, and this was also the comment of referee #2. We have clarified this point with changes throughout the manuscript. In the new version, we explain that we use an assessment approach inspired by the techniques used in Observing System Simulation Experiments (OSSEs) where a numerical simulation is used as ‘true ocean’, which provides both, the observations and the 3D reference field that will be used to assess the results of the reconstruction (as shown in Fig. 2).

AC: There are changes in the abstract, introduction and Sec. 2.1 in order to better explain our main aim and the used approach. The title of the paper has also been changed to: ”3D Reconstruction of Ocean Velocity from HFR and ADCP: a model-based assessment study”, in order to make clearer this aspect of the methodology.

6- *Page 2, line 27: change to “combining simulated information from ”.*

AR: We have changed the full sentence to make it clearer. In fact, we have fully changed this part of the Introduction.

7- *Page 2, line 30: change to “performance”.*

AR: Done.

AC: in page 3, line 6

8- *Page 3, line 17: change to “with surface temperatures over”.*

AR: Done

AC: in page 3, line 20

9- *Page 4, line 1: remove Moreover.*

AR: Done.

AC: in page 4, line 19

10- *Page 5, line 3: replace Summarizing with In summary,*

AR: Done.

AC: in page 5, line 18

11- *Page 5, line 11: change to "surface current fields along the Mid Atlantic".*

AR: Done.

AC: in page 5, line 26

12- *Page 6, line 19: can the authors be more specific on what is meant by the observations and the reference fields.*

AR: When dealing with methods for data 3D reconstruction, what we need to evaluate is the solution in the whole 3D domain, and namely in the areas that are not close to the observations. To this end, as explained in comment *5,* we use an assessment approach inspired by the techniques used in Observing System Simulation Experiments (OSSEs), where the observations that are used as inputs for the methods are emulated by a numerical simulation, and then the outputs (the reconstructed fields) are compared to the reference field obtained also from the 'true ocean' that is provided by such simulation. This approach is now better explained in Sect. 2.1 and different modifications through all the manuscript have been addressed accordingly.

13- *Page 7: What data source was used for the correlation scale tests, IBI, GLORYS-HR or GLORYS-LR?*

AR: The analysis of Sect. 3.1 (now changed to Sect. 3) provides an overview of the characteristics of the currents simulated by the numerical simulation from where the 'true' ocean was extracted. The IBI dataset was used for this purpose since as explained in this section, it has proven to be a realistic numerical simulation.
This change of Sect. 3.1 to Sect. 3 was made in order to make the manuscript clearer. In addition, note that the first paragraph of Sect. 2.3, where the numerical simulations are described, also links that section to this one.

AC: the initial configuration of the sections has been changed as mentioned, in addition to some changes throughout Sect. 3.

14- *Page 9: Figs 10-11 are mentioned before Figs 6-9, can this be changed.*

AR: Thank you, you are right.

AC: We have moved this paragraph to the end of the section as a general conclusion. Page 10, lines 20-24.

15- *Page 12, line 6: change to "the combination of synthetic data that mimics sensors from a multiplatform observing system to reconstruct".*

AR: We have changed the full paragraph to make clearer that we use emulated observations based on a realistic scenario as explained in the response to the comments before.

AC: in page 11

Anonymous Referee #2

Referee's Comments

I went through the manuscript with great interest as the data-driven reconstruction of subsurface velocity is a topic of grea interest and has some potential but I must admit I was disappointed when reading the body of the text. the title and the paper are misleading as they suggest that real data are used for the task, which unfortunately is not the case here. The manuscript indeed focuses on 'emulated' observations of currents provided through some 'supposedly' accurate and realistic model simulation. However, when it comes to the description of the model, the reader is pointed out to some references to other studies. If you have the model, why not compare that to the HFR data if you do not want to use the data itself for the task?

the literature review is lacking some important references. Development of subsurface current estimation procedures to complement surface currents started as soon as radar technologies were available. Some are given below, I leave the Authors to do a thoroughly review. Simple models dedicated to the prediction of current profiles have been developed (Prandle D., 1982. The vertical structure of tidal currents. Geophysical and Astrophysical Fluid Dynamics, 22, 29-49, 1982. Prandle D., 1987. The fine-structure of nearshore tidal and residual cirrculatins revealed by HF radar surface current measurements. Journal of Physical Oceanography, 17, 231-245, 1987. Prandle D., 1991. A view of near-shore dynamics based on observations from HF radar. Progress in Oceanography, 27, 403-438, 1991. ; Davies, 1982, 1983, 1985, 1992). Semi-empirical models, based on shallow-water hydrodynamics coupled to a modal representation of the current profiles, in which the modes have been estimated from local current profiles time series, have been used to estimate the 3-dimensional flow field from HF surface currents near the Rhine river outflow (de Valk C.F., 1999. Estimation of the 3-D current fields near the Rhine outflow from HF radar surface current data. Coastal Engineering, 37, 487-511, 1999.). A statistical method, based on vector correlation analysis between HF surface and ADCP subsurface currents and coupled with a modal representation in which modes were obtained from ADCP currents, was proposed in order to "project" surface currents along the water column. A different approach that infers the approximate shape of the current profiles from surface data without making use of lo-cal current profiles, has been introduced in 2001 for shallow-water coastal zone (Shen et Evans, 2001), subsequently extended to deep-water regions (Shen C.Y., Evans T., 2001. Surface-to-subsurface velocity projection for shallow water currents. Journal of Geophysical Research, 106, C4, 6973-6984, 2001. Shen C.Y., Evans T., 2002. Dynamically constrained projection for subsurface current velocity. Journal of Geophysical Research, 107, C11, 3203-3216, 2002. Doi: 10.1029/2001JC001036.), and is meant as an alternative to data assimilation into circulation models. The same approach has been recently applied to a shallow-water region in order to infer current profiles and to obtain maps of sea-surface slope from HF radar current estimates (Marmorino G.O., Shen C.Y., Evans T., Lindemann G.J., Hallock Z.R., Shay L.K., 2004. Use of 'veloc-ity projection' to estimate the variation of sea-surface height from HF Doppler radar current measurements. Continental Shelf Research, 24, 353-374, 2004.). More re-cently, coupled with a two-layer density plume model, this technique was applied to estimate current profiles and

density structure in a coastal zone dominated by a plume (Gangopadhyay A., Shen C.Y., Marmorino G.O., Mied R.P., Lindeman G.J., 2005. An extended velocity projection method for estimating the subsurface current and density structure for coastal plume regions: an application to the Chesapeake Bay outflow). The so-called “Velocity Projection Technique” introduced in these papers, relies on the surface-to- subsurface viscous coupling and turbulent transfer of momentum and shear in order to infer the velocity distribution over depth from measured surface currents and wind stress. This method, applied in its original formulation to shallow coastal water, re-solves the vertical structure of the currents in terms of a finite expansion of orthogonal modes spanning the water column. The modal weights are obtained by applying appropriate dynamical constraints to the inferred current profiles and their vertical derivatives at the boundaries.

Abstract / main body: define surface. HFR sense different ’depths’ based on the working frequency. Define Long-Range and spell "ADCP’. Although I am puzzled by the fact that ’no real data is used for this paper’ some details should be given on the HFR systems mentioned here.

two methods are introduced here and the abstract mentions that one seems to perform better than the other one - please provide quantitative information so to guide other users in their choice and critically assess the reasons why one method is performing better than the other.

Introduction. lines23-27: I don’t understand this sentence. it seems to me that you are using horizontal interpolation (as described in the cited references) to reconstruct the vertical profile - which is not the case here. please rephrase this (and other sentences in the ms, possibly with the help of a native English speaking service- as most of the sentences are long and convoluted and can be misinterpreted.

Section 2.2 Please provide quantitative figures of data reconstruction accuracy - even from different deployments as long as other readers have a clear idea of what we’re aiming at here.

Skill assessment: this is done at a very basic level. there’s plenty of good skill assessment approaches that would be more appropriate than what is used here.

Section 3.1. This needs to be rewritten in a more understandable way.

Section 3.2. define winter and summer seasons.

Overall, I think it has potential, but, I am puzzled and at this stage I am choosing to reconsidr after major revisions although I am leaning towards rejection. no real data is used -apart from the initialization of the covariance matrix, which should have been derived through HFR data instead. Using real data is complicated, fair enough, but this would guide users to a feasibility study in a more realistic scenario: what is the effect of data gaps, what is the data output rate that should be used (hourly-daily-weekly averaged HFR currents?). There is no discussion of the proposed approaches against data assimilation into the model, which has proven a very effective way of correcting a model’s trajectory. there is no discussion of the computational requirements or efforts, again for instance against data assimilation into the models. If the proposed

approaches are more effective (machine time - wise for instance) well that's would be beneficial indeed.

Author's comments

Dear reviewer,
Thank you for your thorough and critic review of our manuscript. Reading your comments, we have realized that neither the main idea nor the approach used to carry out our investigation were clear. Therefore, we have made significant changes throughout all the manuscript to correct these aspects and improve the readability of the paper. We are also very grateful for your suggestions on the literature cited in the paper and for providing additional context in terms of references. We hope that thanks to your suggestions we have managed to improve the manuscript, and that it suits now the standards of Ocean Science. The point by point response to your comments and the related changes are detailed in the following.
Best regards,
Ivan Manso

AR = Author's response
AC = Author's changes in the manuscript

General response:
AR = We deeply thank the reviewer for his/her comprehensive review of the manuscript and the very helpful comments. Indeed, we realized that our explanation on the approach used for the analysis of the methods' skills was not clear enough, and we have thoroughly rewritten several parts of the manuscript to correct this important aspect.
We agree with the reviewer that the most interesting aspect about the data-reconstruction methods is their application on real data. What we propose in this paper is a methodology for the evaluation of the 3D reconstruction methods prior to their application to real data. Our approach is based on the use of realistic numerical simulations as a 3D "true" ocean, that provides both, the observations and the 3D reference field that will be used to assess the results of the reconstruction ("reference field"). This is a well-established approach inspired by the techniques used in Observing System Simulation Experiments (OSSEs) and is the only approach that allows to test the methods in the full 3D domain considered for the reconstruction.
Performing a complete evaluation of the reconstructed fields would not be possible using only real observations, since it would be limited only to the areas covered by the observing systems. When dealing with methods for 3D data-reconstruction, what we need to evaluate is the solution in the whole domain, and namely in the areas that are not close to the observations.
In our opinion, this study is an essential prior step towards the applicability of this kind of methods on real data. Despite that the skill assessment approach is straightforward, it provides the ground information and conclusions needed (i.e. where and why each method performs better/worse and their limitations) to know whether the application of the methods is feasible or not. We also think that the best-practice methodology developed in this work can be easily transferable to other locations and study cases, and prove very useful for expanding the use of 3D reconstruction on HFR observations.

The numerical simulation used as “true” ocean has proven to be realistic and in agreement with real data (in response with the reviewer’s suggestions, this is now explicitly discussed in Sect. 3). We consider that the good agreement with the observations validates the approach used here and the conclusions obtained for our study area.

AC = After considering the comments of the two anonymous referees, major changes have been made in the manuscript. First, we have better defined the context of this work using, among others, the references proposed by referee#2. The introduction of these references results in a more complete introduction, with regard to studies for the expansion of HFR data to subsurface levels. We have also changed the Sect. 3.1 into Sect. 3 separating it from the main results (now in Sect. 4); thus, leaving its own section to the description of the simulated “true” ocean. We have also clarified the main aim, approach and conclusions of our work, with changes in several parts of the manuscript which are detailed in the following point by point responses.

Point by point responses:
Comments are enumerated.

1- *the title and the paper are misleading as they suggest that real data are used for the task, which unfortunately is not the case here.*

   AR: You are right, thanks for the comment. We have changed the title accordingly to provide a better idea on what it is done in this study.

   AC: the new title is ”3D Reconstruction of Ocean Velocity from HFR and ADCP: a model-based assessment study”

2- *The manuscript indeed focuses on ’emulated’ observations of currents provided through some ’supposedly’ accurate and realistic model simulation. However, when it comes to the description of the model, the reader is pointed out to some references to other studies. If you have the model, why not compare that to the HFR data if you do not want to use the data itself for the task?*

   AR: First of all, sorry for not being clear with regard to the explanation of our main approach and the description of the model used to emulate the reality as “true” ocean (as explained in the general response). As mentioned before, to assess the results of the reconstruction we need a 3D “ground truth” that can be used to compare the different methods. And we need it with a good spatiotemporal coverage, which in practice can only be provided by numerical models. Then, it is important to be sure that the model is realistic enough, so the evaluations are meaningful. By realistic we mean that the model has to reproduce the dominant processes in the region (i.e. permanent currents, mesoscale structures) so the spatiotemporal correlations among different locations are close to the actual ones.
   In order to improve this aspect, a new section (Sect. 3) has been created from the former Sect 3.1, and it is used for assessing the realism of the simulations through their validation with previous studies based on observations in the study area (Rubio et al. (2013, 2019) and Solabarrieta et al. (2014)).

AC: We have changed Sect. 3.1 into Sect. 3 (and rearranged the following sections accordingly) adding more discussion concerning the validation of the simulations. We have also added a paragraph in Sect. 2.3 (page 6 lines 20-22) to connect section 2.3 and the new Section 3.

3- *the literature review is lacking some important references. Development of subsurface current estimation procedures to complement surface currents started as soon as radar technologies were available. Some are given below, I leave the Authors to do a thoroughly review. Simple models dedicated to the prediction of current profiles have been developed (Prandle D., 1982. The vertical structure of tidal currents. Geophysical and Astrophysical Fluid Dynamics, 22, 29-49, 1982. Prandle D., 1987. The fine-structure of nearshore tidal and residual cirrculatins revealed by HF radar surface current measurements. Journal of Physical Oceanography, 17, 231-245, 1987. Prandle D., 1991. A view of near-shore dynamics based on observations from HF radar. Progress in Oceanography, 27, 403-438, 1991. ; Davies, 1982, 1983, 1985, 1992). Semi-empirical models, based on shallow-water hydrodynamics coupled to a modal representation of the current profiles, in which the modes have been estimated from local current profiles time series, have been used to estimate the 3-dimensional flow field from HF surface currents near the Rhine river outflow (de Valk C.F., 1999. Estimation of the 3-D current fields near the Rhine outflow from HF radar surface current data. Coastal Engineering, 37, 487-511, 1999.). A statistical method, based on vector correlation analysis between HF surface and ADCP subsurface currents and coupled with a modal representation in which modes were obtained from ADCP currents, was proposed in order to "project" surface currents along the water column. A different approach that infers the approximate shape of the current profiles from surface data without making use of local current profiles, has been introduced in 2001 for shallow-water coastal zone (Shen et Evans, 2001), subsequently extended to deep-water regions (Shen C.Y., Evans T., 2001. Surface-to-subsurface velocity projection for shallow water currents. Journal of Geophysical Research, 106, C4, 6973-6984, 2001. Shen C.Y., Evans T., 2002. Dynamically constrained projection for subsurface current velocity. Journal of Geophysical Research, 107, C11, 3203-3216, 2002. Doi: 10.1029/2001JC001036.), and is meant as an alternative to data assimilation into circulation models. The same approach has been recently applied to a shallow-water region in order to infer current profiles and to obtain maps of sea-surface slope from HF radar current estimates (Marmorino G.O., Shen C.Y., Evans T., Lindemann G.J., Hallock Z.R., Shay L.K., 2004. Use of 'velocity projection' to estimate the variation of sea-surface height from HF Doppler radar current measurements. Continental Shelf Research, 24, 353-374, 2004.). More recently, coupled with a two-layer density plume model, this technique was applied to estimate current profiles and density structure in a coastal zone dominated by a plume (Gangopadhyay A., Shen C.Y., Marmorino G.O., Mied R.P., Lindeman G.J., 2005. An extended velocity projection method for estimating the subsurface current and density structure for coastal plume regions: an application to the Chesapeake Bay outflow). The so-called "Velocity Projection Technique" introduced in these papers, relies on the surface-to- subsurface viscous coupling and turbulent transfer of momentum and shear in order to infer the velocity distribution over depth from measured surface currents and wind stress. This method, applied in its original formulation to shallow*

coastal water, resolves the vertical structure of the currents in terms of a finite expansion of orthogonal modes spanning the water column. The modal weights are obtained by applying appropriate dynamical constraints to the inferred current profiles and their vertical derivatives at the boundaries.

AR: Thank you very much for providing additional context in term of references about studies that investigate procedures to expand surface HFR information to subsurface levels. We have rewritten part of the Introduction accordingly.

AC: We have changed part of the introduction (page 2, line 24 – page 3, line 2):
"In the last years, several methods to expand the information of the HFR data to subsurface layers in the upper water column have been developed, such as: the use of multifrequency radars to obtain the velocity shear (Stewart and Joy, 1974; Barrick, 1972; Broche et al., 1987; Paduan and Graber, 1997; Teague et al., 2001), the use of the secondary peaks in the radar echo spectra to obtain the velocity shear (Shrira et al., 2001; Ivonin et al., 2004) or the "velocity projection" method to obtain the velocities of the subsurface currents (Shen and Evans, 2002; Marmonio et al., 2004; Gangopadhyay et al., 2005). Besides, simple models that study the surface and vertical profiles have been developed (e.g. Prandle, 1982, 1987, 1991; Davies, 1985a, 1985b, 1985c). In addition, other approaches combine the HFR data with data in the water column provided by in-situ moored instruments, remote sensing platforms or circulation numerical simulations to investigate the 3D circulation (e.g. C.F. de Valk, 1999; O'Donncha et al., 2014; Cianelli et al., 2015; Ren et al., 2015; Jordà et al., 2016; Fredj, 2016)."

4- *Abstract / main body: define surface. HFR sense different 'depths' based on the working frequency. Define Long-Range and spell "ADCP'. Although I am puzzled by the fact that 'no real data is used for this paper' some details should be given on the HFR systems mentioned here.*

AR: Modified.

AC: Surface defined in page 2 line 19. ADCP spelled in page 3 line 6. Details of the HFR used to define the numerical-based scenario for this work are now given in page 3 line 23.

5- *two methods are introduced here and the abstract mentions that one seems to perform better than the other one - please provide quantitative information so to guide other users in their choice and critically assess the reasons why one method is performing better than the other.*

AR: In the abstract it is mentioned that in general the methods perform better in well sampled areas and that both show different performances. However, it was not our aim to say that one is better than the other. In order to make it clearer we have removed the phrase where we said that different performances were observed between them.
Actually, as explained in the conclusions section, each method has its pros and cons and it is difficult to summarize them in the abstract. In Sect. 4.1, where the results are presented,

it is shown that the DCT-PLS performs better in well sampled areas whereas the ROOI performs better in the rest of the areas, although it also performs well in well sampled areas.

AC: We have removed the phrase "although different performances between the methods are observed". The whole abstract has been revised to improve clarity on the aim, methods and results of our work.

6- *Introduction. lines23-27: I don't understand this sentence. it seems to me that you are using horizontal interpolation (as described in the cited references) to reconstruct the vertical profile - which is not the case here. please rephrase this (and other sentences in the ms, possibly with the help of a native English speaking service- as most of the sentences are long and convoluted and can be misinterpreted.*

AR: We agree with that this sentence was confusing. We have changed the part of the introduction where the methods for inferring sub-surface currents are described and where the methods that we use are introduced. We hope that now it is clearer. English language has been reviewed through all the manuscript, sentences have been shortened and simplified when needed.

AC: The main change in the introduction is made between page 2, line 24- page 3, line 10.

7- *Sect. 2.2 Please provide quantitative figures of data reconstruction accuracy – even from different deployments as long as other readers have a clear idea of what we're aiming at here.*

AR: Thank you, this is an interesting point. However, it is not easy to compare the cases of those applications with our case since the data, study area and configurations were different. Also, same RMSD, for instance, can have a very different meaning depending on the characteristics of the circulation in each region. In any case if the reader is interested in those results, they can now be found in the references.

8- *Skill assessment: this is done at a very basic level. there's plenty of good skill assessment approaches that would be more appropriate than what is used here.*

AR: We agree that there are plenty options of the skill assessment of the methods, both from the eulerian or the lagrangian perspective. However, it is also true that the RMSD (and relative RMSD) is an intuitive quantity that provide a first evaluation of the error in the same units as the variable being evaluated (or as a percent to its variability). Other complementary diagnostics could have been used (and were tried in a previous version of the manuscript), but they do not provide much further insight while they make the manuscript denser. Therefore, we prefer to stick to the chosen diagnostics that have proven enough to evaluate the benefits and drawbacks of each method. In any case, we put special effort in the computation of the RMSD in different ways by using maps and

spatial and temporal means with the aim to characterise in a comprehensive way the 3D structure of the errors associated to the reconstructed fields.

9- *Sect. 3.1. This needs to be rewritten in a more understandable way.*

AR: Thank you. The whole section has been revised. Sect. 3.1 is now Sect. 3 and sections Sect. 2.4 and 3 are now better connected. We hope that these changes have made this section clearer. Part of the contents have been moved to an appendix in order to ease the reading.

AC: the initial configuration of the sections has been changed as mentioned, in addition to some changes to the main text, now in Sect. 3.

10- *Sect. 3.2. define winter and summer seasons.*

AR: They are already defined in Sect. 2.1: "winter and summer periods: Nov-Dec-Jan-Feb (2010-2011) and Jun-Jul-Aug-Sep (2011), respectively".

11- *no real data is used -apart from the initialization of the covariance matrix, which should have been derived through HFR data instead.*

AR: For the application of the ROOI method we needed to define a 3D velocity covariance matrix (eq. 1). To do this, time series of velocity in each grid point where the reconstruction will be performed, are required. This cannot be achieved from real data, so this matrix was obtained from a realistic model simulation. Note that here the hypothesis is that the statistical relationships between different locations are well captured by the model, which is less demanding than requiring that the velocity field is well reproduced at each time step. Moreover, we have tested the impact of the choice of different numerical simulations for the computation of the 3D velocity covariance matrix (IBI, GLORYS-HR and GLORYS-LR, see Figs 10-11). The goal of this test is to see what would happen if the model used did not totally represent the same dynamics than reality (i.e. the modelled covariance matrix was inaccurate).

12- *Using real data is complicated, fair enough, but this would guide users to a feasibility study in a more realistic scenario: what is the effect of data gaps, what is the data output rate that should be used (hourly-daily-weekly averaged HFR currents?).*

AR: As mentioned before, we do not use real data because 3D reconstructions could not be validated with existing data (i.e. data sampling in subsurface is very scarce). Thus, we work in the "model world" to better identify limitations and skills of the reconstruction methods. However, the reviewer is right in that we could have used a more realistic configuration for instance by adding gaps and errors to the emulated data. Unfortunately, the paper is already long, so we cannot include more sensitivity experiments. Moreover, this has already been addressed in a 2D context by other authors (* e.g. Hernández-Carrasco, 2018; Kaplan and Lekien, 2007; Yaremchuk and Sentchev, 2009). We added a sentence explaining that

it would be an interesting further step to evaluate the robustness of the reconstruction methods when dealing with observational issues.
With regard to the data input rate, for this study hourly data were used. While not limitations on the time resolution exist for the DCT-PLS, the ROOI outputs will be limited to the temporal resolution of the covariance matrix. In a case with real data, the temporal resolution of the reconstruction should be chosen in coherence to the process to be monitored/studied and after examination of the spatio-temporal correlations.

*Hernández-Carrasco, I., Solabarrieta, L., Rubio, A., Esnaola, G., Reyes, E., and Orfila, A.: Impact of HF radar current gap filling methodologies on the Lagrangian assessment of coastal dynamics, Ocean Sci., 14, 827-847, https://doi.org/10.5194/os-14-827-2018, 2018.

Kaplan, D. M., and Lekien, F.: Spatial interpolation and filtering of surface current data based on open-boundary modal analysis, J. Geophys. Res.-Oceans, 112, C12007, https://doi.org/10.1029/2006JC003984, 2007.

Yaremchuk, M., and Sentchev, A.: Mapping radar-derived sea surface currents with a variational method, Cont. Shelf Res., 29, 1711-1722, https://doi.org/10.1016/j.csr.2009.05.016, 2009.

AC: We added a sentence explaining that it would be an interesting further step to evaluate the robustness of the reconstruction methods for different observational errors in page 11 lines 20-21.

13- *There is no discussion of the proposed approaches against data assimilation into the model, which has proven a very effective way of correcting a model's trajectory.*
there is no discussion of the computational requirements or efforts, again for instance against data assimilation into the models. If the proposed approaches are more effective (machine time - wise for instance) well that's would be beneficial indeed.

AR: We thank the reviewer for this suggestion that is useful to clarify the scope of the methodologies. Indeed, the ROOI method shares several characteristics with what is used in data assimilation (DA) methods, in particular in sequential methods like Optimal Interpolation (* Ide et al., 1997) or the SEEK filter (* Brasseur and Verron, 2006). So, the comment is very appropriate.
The main difference between this type of reconstructions and data assimilation is not in the methodology *per se* but in the overall approach. Data assimilation is typically applied to correct a model trajectory. That is, the background field used is a model forecast, that is combined with the information from observations to create an analysed field. This field is then used to initialize the model for the next simulation cycle. In the reconstruction methods we analyse in this work, the 3D velocity field is inferred solely from the observations. Only in the case of ROOI a model is used to provide the covariance matrices, which are fixed in time (i.e. only computed once).
In summary the main differences of these methods with DA are (1) no model has to be run to provide a background field, so the procedure is much faster and (2) most of the information is provided by the observations and the model is only used in the ROOI case to provide background statistics.

* Ide, K., Courtier, P., Ghil, M., and Lorenc, A. C.: Unified Notation for Data Assimilation: Operational, Sequential and Variational (gtSpecial IssueItData Assimilation in Meteology and Oceanography: Theory and Practice). *Journal of the Meteorological Society of Japan. Ser. II*, *75*(1B), 181-189, 1997.

*Brasseur, P., and Verron, J.: The SEEK filter method for data assimilation in oceanography: a synthesis. *Ocean Dynamics*, *56*(5-6), 650-661, 2006.

AC: We have added a sentence showing the added values of the methods compared to data assimilation in the conclusions in page 12 lines 6-8

Marked-up version of the manuscript:

3D~~Three-Dimensional~~ Reconstruction of Ocean Velocity~~Circulation~~ from HFR~~Coastal Marine Observations: Challenges~~ and ADCP: a model-based assessment study~~Methods~~

Ivan Manso-Narvarte[1], Erick Fredj[2], Gabriel Jordà[3], Maristella Berta[4], Annalisa Griffa[4], Ainhoa Caballero[1] and Anna Rubio[1]

[1] AZTI-Marine Research, Pasaia, Spain
[2] Department of Computer Sciences, Jerusalem College of Technology~~technology~~, Jerusalem, Israel
[3] Instituto Español de Oceanografía, Centre Oceanogràfic de Balears, Palma de Mallorca, Spain
[4] ISMAR, CNR, La Spezia, Italy

Correspondence to: Ivan Manso-Narvarte (imanso@azti.es)

Abstract. The effective monitoring and understanding of~~Monitoring and investigating~~ the dynamics of coastal currents is crucial for the development of environmentally sustainable coastal activities, in order to preserve marine ecosystems as well as to support marine and navigation safety. This need is driving the set-up of a growing number of multiplatform operational observing systems, aiming for~~to~~ the continuous monitoring of the coastal ocean. A significant percent of the existing observatories is ~~today~~ equipped with land-based High Frequency Radars (HFRs~~HFR~~), which provide real-time currents with high spatio-temporal~~unprecedent~~ coverage and resolution. Several approaches have been used in the past~~, limited however,~~ to expand the surface current velocity measurements provided by HFR to subsurface levels, since this can expand the application of the technology to other fields, like marine ecology or fisheries.~~layer.~~ The possibility of obtaining 3D velocity current fields from the combination of data from HFRs~~HFR~~ with complementary data as the velocity current profiles provided by~~from~~ in-situ Acoustic Doppler Current Profiler~~platforms providing information of the currents at subsurface layers~~ (ADCP) moorings~~)~~ is explored~~investigated~~ here. To that end, two different methods ~~-~~to reconstruct the 3D current velocity fields are assessed by a standard approach conceptually similar to OSSEs (Observing System Simulation Experiments), where 3D numerical simulations are used as "true" ocean in order to evaluate the performance of the data-reconstruction methods. The ~~field from in-situ~~ observations of currents from a HFR and ADCP moorings are emulated by extracting the corresponding data from the 3D "true" ocean, and used as input for the methods. Then, the 3D reconstructed fields (outputs of the methods) are compared to the "true" ocean to assess the skills of the data-reconstruction methods. These methods are ~~. For this purpose, two methods~~ based on different approaches; on~~ are used. On~~ the one hand, the Reduced Order Optimal Interpolation uses an approximation to the velocity covariances (which can be obtained from historical data or a ~~is fed, in this case, with a spatial covariance matrix~~

~~extracted from a~~ realistic numerical ~~oceanic~~ simulation)~~;~~; and on the other hand, the Discrete Cosine Transform Penalized Least Square, is~~which is a data gap filling method~~ based on penalized least squares regression that balances fidelity to the data and smoothness of the solution. This study, which is based on

~~As a proof of concept, we test~~ the configuration of a ~~methods' skills by using emulated observations of currents, extracted from a numerical simulation (3D reference field). The test set up emulates the~~ real observatory located~~scenario~~ in the ~~study area (~~south-eastern Bay of Biscay (SE-BoB), is a first step towards the application of the data-reconstruction methods to real data, since it provides the procedure to explore their skills and limitations. In the SE-BoB, where the coastal observatory~~),~~ ~~which~~ includes a long-range HFR and two ADCP moorings inside the HFR footprint area~~. Then, the reconstructed fields (outputs of the methods) are compared with the 3D reference fields. In general~~, the results show satisfactory 3D reconstructions with mean spatial (for each depth level) errors between 0.55–7~~10.94~~ cm s^{-1} for the first 150 m depth and mean relative errors of 0.07–1.2 times the RMS, for most of the cases . The data-reconstruction~~. The~~ methods perform better in well sampled areas, and ~~although different performances between the methods are observed,~~ both show promising skills for the 3D reconstruction of currents as well as for the computation of new operational products integrating complementary observations, broadening the applications of the in-situ observational data in the study area.

1 Introduction

Multiplatform observing systems are arising in several areas of the coast for providing data at different spatio-temporal scales. The combination of such data is a powerful approach for a better monitorization and understanding of the 3D coastal circulation, which is a key aspect to support sustainable coastal activites~~marine and navigation safety~~, as well as to preserve marine ecosystems.

Among the different observing systems, High Frequency Radar (HFR) technology offers a unique insight into coastal ocean variability, by providing information at~~of~~ the ocean~~ and~~ atmosphere interface. It allows~~for~~ a better understanding of the coupled ocean-atmosphere system and the surface ocean coastal dynamics. In addition, since HFR data can provide real-time measurements of currents with a relatively wide spatial coverage (up to 200 km from the coast) and high spatial and temporal resolution (typically a few km and one hour)~~,) in near real time,~~ they have become invaluable tools in the field of operational oceanography. Recent reviews on this technology and its applications worldwide have been provided by several authors (Fuji et al., 2013; Paduan and Washburn, 2013; Wyatt, 2014, Rubio et al., 2017; Roarty et al., 2019). However, HFRs provide current data only relative to the surface, within an integration depth ranging from tens of cm to 1–2 m~~,~~ depending on the operating frequency (see Rubio et al., 2017). Moreover, data coverage is not always regular and may contain spatial and temporal data gaps due to several environmental, electromagnetic and geometric causes (Chapman et al., 1997).

The propagation~~combination~~ of HFR information along~~data with complementary data of coastal currents in~~ the water column is especially valuable as~~useful since~~ it may broaden~~enables to increase~~ the application of this technology~~temporal and spatial coverage and expand the information towards subsurface layers, broadening their application~~ to biological, geochemical and

environmental issues, since plankton or pollutants can be located deeper in the water column and not only follow surface dynamics. In the last years, several methods to expand the information of the HFR data~~Nevertheless, the combination of independent measurements of the ocean surface currents with those along the water column is challenging since the surface and the water column dynamics may respond~~ to subsurface layers in the upper water column~~different forcing and can be characterized by different space and time scales. Moreover, the measurements at the surface and in the water column are done under different observation principles and may have different space and time coverage and resolution.~~

~~Several data gap filling/reconstruction methods such as the ones in Table 1~~ have been developed, such as: the use of multifrequency radars~~widely used in different studies applied~~ to obtain the velocity shear (Stewart and Joy, 1974; Barrick, 1972; Broche~~oceanographic data sets (e.g. Yaremchuk and Sentchev, 2009; Hernández-Carrasco~~ et al., 1987; Paduan and Graber, 1997; Teague~~2018; Taillandier~~ et al., 2001), the use of the secondary peaks in the radar echo spectra to obtain the velocity shear (Shrira et al., 2001; Ivonin et al., 2004) or the "velocity projection" method to obtain the velocities ~~2006; Jordà et al., 2016; Fredj et al., 2016; Esnaola et al., 2013; Alvera-Azcárate et al., 2007; Barth et al., 2014). In this work we aim to explore the use of two~~ of ~~them for the 3D reconstruction of high resolution coastal current fields by combining information from one long-range HFR and two moorings equipped with ADCPs providing data every 8 meters from~~ the subsurface currents (Shen and Evans, 2001, 2002; Marmonio et al., 2004; Gangopadhyay et al., 2005). Besides, simple models that study the surface and vertical profiles have been developed (e.g. Prandle, 1982, 1987, 1991; Davies, 1985a, 1985b, 1985c). In addition, other approaches combine~~surface to ~150 m depth inside~~ the HFR data with data in the water column provided by in-situ moored instruments, remote sensing platforms or circulation numerical simulations to investigate the 3D circulation (e.g. De Valk, 1999; O'Donncha et al., 2014; Cianelli et al., 2015; Ren et al., 2015; Jordà et al., 2016).

In line with these approaches, in this work we explore the ~~footprint area. Hence, the~~ skills of two data-reconstruction methods that allow to expand the surface information to subsurface layers by reconstructing 3D current fields from the combination of observations that provide complementary spatial coverage, and in particular to those obtained from a long-range HFR and two moorings equipped with Acoustic Doppler Current Profilers (ADCPs). The ~~are assessed and compared, aiming to give a first step towards their applicability for this specific case. These~~ two methods used here have already shown~~were chosen because of their~~ good performance~~performances in previous attempts~~ for the reconstruction of HFR current data and ~~because they~~ rely on different basic principles. On the one hand,~~:~~ the Discrete Cosine Transform Penalized Least Square (DCT-PLS), implemented by Fredj et al. (2016), is based on the fitting of a function. On the other hand,~~, and~~ the Reduced Order Optimal Interpolation (ROOI), implemented by Jordà et al. (2016), uses an approximation to the velocity covariances to extrapolate observed information to the whole domain. ~~. The assessment of the performances of both methods is carried out in terms of current velocities, using a scenario based on a real observatory located at the south eastern Bay of Biscay (SE BoB) (Fig. 1a). To that aim, a synthetic reality experiment is performed. In particular, the outputs of a realistic numerical simulation in the study area are used as synthetic reality from which observations are extracted (emulating data from one HFR and two ADCPs moored inside the HFR footprint area). The results are then compared to the original numerical simulation outputs (reference field) to evaluate the quality of the reconstructed fields and quantify the methods' skills.~~

~~2 Methods and data~~

~~2.1 Study area and main approach~~

The study area is located in the south eastern Bay of Biscay (SE-BoB)~~,~~ which is characterized by the presence of canyons (e.g. Capbreton canyon), by an abrupt change in the orientation of the coast and by a narrow shelf ~~and slope~~ (see Fig. 1). The winter surface circulation in the SE-BoB is mainly related to a slope current flowing, in the upper 300 m of the water column, eastwards along the Spanish coast and northwards along the French coast (the so-called Iberian Poleward Current, IPC) (Frouin et al., 1990; Haynes and Barton, 1990; Pingree and Le Cann, 1990, 1992a, 1992b; Peliz et al., 2003; Le Cann and Serprette, 2009) with maximum surface current speeds~~currents~~ of 70 cm s^{-1} (Solabarrieta et al., 2014). In summer, the surface flow is reversed being three times weaker than in winter (Solabarrieta et al., 2014). In the water column, the sub-surface properties measured by two slope moorings~~buoys~~ show a marked seasonal variability (Rubio et al., 2013). Whilst in winter, the water column is well-mixed and shows stronger currents (strongest currents ranging from 20 cm s^{-1} to 50 cm s^{-1}), in summer, it is stratified with mean thermocline depths ranging from -30 to -50 m, with surface temperatures over 20 °C and with weaker currents (strongest currents ranging from 10 cm s^{-1} to 20 cm s^{-1}).

The multiplatform coastal currents observatory~~observing system available~~ in this study area belongs to the Basque Operational Observing System (EuskOOS, www.euskoos.eus) and is composed by one long-range HFR (working at a central frequency of 4.5 MHz with an integration depth of ~1.5 m depth and with a footprint area that covers ~150 km off the coast) and two ~~). For this study, two current vertical profiles emulating the data obtained by~~ ADCPs located in two slope moorings~~buoys~~ (Matxitxako and Donostia moorings~~buoys~~) along the Spanish coast.

The assessment of the performances of the data-reconstruction methods is carried out in terms of current velocities, using a model-based scenario based on the coastal observatory existing in the study area. Thus, the skills of two data-reconstruction methods are assessed and compared, aiming to give a first step towards their applicability for this specific case.

2 Methods and data

2.1 Assessment approach

The approach used for the analysis of the data-reconstruction methods' skills is based on the use of a ~~, and surface currents fields emulating the fields obtained by a HFR were extracted from a~~ realistic numerical simulation as a "true" ocean, that provides both, the ~~. The~~ emulated observations and the 3D reference field (hereinafter "reference field") that will be used to assess the results of the 3D reconstruction. This is a well-established methodology inspired by the techniques used in Observing System Simulation Experiments (OSSEs) and is the only approach that allows to quantify the skills of the data-reconstruction methods in the entire 3D domain considered for the reconstruction. The assessment approach consisted in three main steps (Fig. 2). First, the observations that emulate the data obtained from the EuskOOS platforms were extracted from a numerical simulation (for simplicity these "emulated observations" are called "observations" from here on). The extracted simulation

data emulate the two vertical current profiles of the ADCPs located in the Matxitxako and Donostia moorings, and the surface current fields of the HFR (see ~~coverage area and the~~ locations and coverage~~of the emulated slope buoys are shown~~ in Fig. 1b). Second, the two data-reconstruction methods were applied to the observations to compute the 3D reconstructed fields. Note that, the ROOI method also uses historical data from a simulation to estimate the spatial covariances of the currents in the study area needed for the reconstruction. Finally, the 3D reconstructed fields (outputs of the methods) were compared to the reference field to assess the performances of the data-reconstruction methods. ~~.~~

Since the current regime is seasonally modulated, the performances of the two data-reconstruction methods were tested for winter and summer periods: Nov-Dec-Jan-Feb (2010-2011) and Jun-Jul-Aug-Sep (2011), respectively.

The data-reconstruction methods were also analysed in a reduced grid case to evaluate the performance of the reconstructions in areas where the surface currents are ~~of~~ highly correlated with~~currents to the observations. Note that in this study these areas generally correspond to~~ the currents at the mooring locations (~~closest points to the observations, therefore,~~ hereinafter ~~these areas will be~~ called "well-~~-~~sampled areas"). Since~~. This reduced grid was determined by~~ the moorings are located along the Spanish slope,~~area~~ where the ~~reference fields' surface~~ zonal current velocity component (U) prevails over the meridional component (V), the reduced grid was determined only by the correlations obtained for this component (~~temporal~~ cross-correlation ~~≥values, between the ADCP locations and the rest of the grid, are higher or equal to~~ 0.8). This reduced grid ~~. Note that this grid is slightly different for each season, however, it~~ mainly covers the Spanish slope area and slightly differs for the winter and summer periods (~~(grids delimited by~~ black and orange lines, respectively, in Fig. 1b). ~~The meridional current velocity component (V) was not considered for determining this grid since U is the velocity component that dominates the current regime at the nearby areas of the ADCP locations.~~

A~~Moreover, a~~ second scenario with two additional current vertical profiles ~~(4 buoy scenario)~~ along the French slope (see Fig. 1b) was also considered in order to assess the sensitivity of the data-reconstruction methods to different observational configurations (hereinafter called "4-mooring scenario"). ~~.~~

~~The approach used for the analysis of the reconstructions is as follows (see Fig. 2): first, the outputs of a numerical simulation were used to extract the observations that emulate the data obtained from a real coastal observatory scenario. These observations were then used as inputs for the data-reconstruction methods. Note that, in addition, the ROOI uses historical data as input to define spatial covariances. Finally, the 3D reconstructed fields were compared to the original outputs of the numerical simulation (reference field) to assess the performances of the data-reconstruction methods.~~

~~-~~2.2 Data-reconstruction methods

2.2.1 The ROOI method

The ROOI method was first proposed by Kaplan et al. (1997) to reconstruct sea surface temperatures (SST) from sparse data and has been applied since then for different variables ~~-~~such as sea level pressure (Kaplan et al., 2000), sea level anomalies (Church and White, 2006), or 3D velocity fields (Jordà et al., 2016). It is based on Empirical Orthogonal Function (EOF)

decomposition and the details can be found in Kaplan et al. (1997, 2000) or Jordà et al. (2016), so here only the basic elements are presented.

Expressing the 3D velocity field as a matrix $Z(r,t)$, where r is the m-vector of spatial locations and t the n-vector of times, a spatial covariance matrix is first computed as $C = n^{-1}ZZ^T$. Then, an EOF decomposition can be applied:

$$C = U\Lambda U^T \quad (1)$$

where U is an mxm matrix whose columns are the spatial modes (EOFs) and Λ is the mxm diagonal matrix of eigenvalues. The velocity field can then be exactly reproduced as:

$$Z(r,t) = U(r) \cdot \alpha(t) \quad (2)$$

in which α can be computed as $\alpha = U^T Z$.

In practice, the velocities at every grid point of the 3D analysis grid are not known, but only at a limited set of N locations, being usually $N << m$. The problem we intend to solve is precisely that of retrieving the whole matrix Z from the available observations (e.g. surface velocities from HFR and velocity profiles at the ADCP locations). The first problem is that the eigenvector U and eigenvalue Λ matrices cannot be computed from actual observations (i.e. there are not enough samples), so a common choice is to use historical data from a realistic numerical simulation to represent the actual velocity statistics. A second aspect to be considered is that fitting high order modes may introduce unwanted noise in the reconstruction. Thus, the Eq. (2) is truncated to include only the M leading EOFs, so that the contribution of the higher-order modes (accounting for local, small-scale features) is neglected:

$$Z_M(r,t) = U_M(r) \cdot \alpha_M(t) \quad (3)$$

The next problem is that obviously the amplitudes cannot be obtained as in Eq. (2), since now we do not know Z. Instead, the M amplitudes can be determined under the constraint that the reconstructed Z_M fits the observations available at each time step. More generally, the amplitudes are obtained minimizing a cost function that takes into account the observational noise and the role of neglected modes (see Kaplan et al., 1997, 2000, for the complete derivation).

In summary~~Summarizing~~, using the ROOI, the values of the velocity at every grid point of a predefined 3D grid can be obtained merging the spatial modes of variability computed from a realistic numerical simulation (used as historical data) and the temporal amplitudes obtained using the available observations. Several sensitivity tests have been performed to tune the method and finally 20 modes have been considered (M=20). Regarding the spatial modes of variability, they have been obtained from different numerical simulations (see Sect. 2.3) to test the sensitivity of the results to the accuracy in the definition of the spatial covariances.

2.2.2 ~~DCT-PLS method~~

The DCT-PLS method

The DCT-PLS method is a straightforward technique~~data gap-filling method~~ proposed by García (2010), based on a penalized least square regression. Fredj et. al. (2016) showcased~~has shown that~~ the method's skills for ~~method is capable of filling data~~

~~gaps in~~ the 2D reconstruction of HFR surface current fields~~networks~~ along the Mid ~~mid-~~Atlantic coast of the United States with high accuracy. ~~Here it is used for filling current data from emulated HFR and ADCP fields in a 3D grid in the SE BoB.~~ In this section the basic principle of the method is explained, however, for more details the reader is referred to García (2010) or Fredj et al. (2016).

The main aim of the method is to find the best fitting model, which is based on Discrete Cosine Transforms (DCTs) and one smoothing (fitting) parameter s. Thus, the fitting model that correspond to each s is tested by cross-validation in order to obtain the best one. The general approach of the method is as follows: for each s (i.e. for each fitting model) the observations are split into two subsets, the training set, which is used to fit the model, and the test set, which is used to test it. This test is carried out by the trade-off (F) between the bias of the fitting (residual sum of squares RSS) and the variance of the results of the created model (penalty term P):

$$F = RSS + P = \|y - \hat{y}\|^2 + s\|D\hat{y}\|^2 \quad (4)$$

where y is the data of the test set, $\hat{y}$ is the data of the created model and D is a second order difference derivative. Then, for the same s, this procedure is repeated for different training and test sets obtaining different F values at each time. The mean value of F (that is, $E[F]$) will provide a General Cross Validation (GCV) score that correspond to each fitting model (i.e. to each s):

$$E[F] \rightarrow GCV \quad (5)$$

, and the best fitting model will be the one that minimizes the GCV score:

$$\min(GCV) \rightarrow s. \quad (6)$$

In conclusion, here we introduce a penalized least square method, based on ~~4D~~ discrete cosine transforms, with one smoothing parameter approach consisting of minimizing a criterion that balances the fidelity with the current data, measured by the RSS, and a P that reflects the noisiness of the smooth current data.

2.3 Numerical simulations

The Atlantic-Iberian Biscay Irish simulation, and particularly the IBI_REANALYSIS_PHYS_005_002 product (hereinafter IBI), provided by the Copernicus Marine Environment Monitoring Service (CMEMS), was used to obtain the "true" ocean from which the observations and the reference field were extracted, as explained in Sect. 2.1~~fields~~. The IBI reanalysis is based on a realistic configuration of the NEMO model for the Iberian Biscay Irish region (Fig. 1a), which~~) that~~ assimilates in situ and satellite data. For more details see Table 1~~2~~ and a complete description about the product and its validation can be found in Sotillo et al. (2015) and the links shown in Table 1. In Sect. 3, the realism of IBI simulations are assessed based on previous knowledge of the circulation in the area and used to provide an overview of the dynamical characteristics of the study area to support the discussion of the results.~~2.~~

The ~~For the ROOI the definition of the~~ spatial covariances ~~is~~ required for the ROOI have~~and, in our case, it has~~ been obtained from IBI and two additional ~~outputs from~~ numerical simulations (see Fig. 2) with daily outputs~~data~~ from 1993 to 2009, with

the objective of exploring the impact on the reconstruction of an imperfect definition of the covariances. The two additional~~. In particular, in addition to IBI, two different~~ numerical simulations ~~were~~ used for this purpose were: the GLORYS high resolution (~~HR) product (~~GLOBAL_REANALYSIS_PHY_001_030 product, ~~) (~~hereinafter called "GLORYS-HR"),~~),~~ and ~~a GLORYS~~ low resolution (~~LR) product (~~GLOBAL_REANALYSIS_PHY_001_025 product, ~~) (~~hereinafter called "GLORYS-LR") reanalyses.~~).~~ The general details of these products are listed in Table 1,~~2~~ along with links to additional information about the products and their validation. ~~The goal of using different simulations is to explore the impact of having an imperfect definition of the covariances.~~ Thus, the ROOI method was tested both in an optimal configuration, where the covariance matrix was obtained from the same numerical simulation used as the reference (i.e.~~ROOI with~~ IBI), and in two suboptimal configurations: one in which the covariances were obtained from a high resolution numerical simulation (i.e.~~ROOI with~~ GLORYS-HR), which is supposed to capture the same range of processes than IBI although not exactly, and another one from a low resolution numerical simulation (i.e.~~ROOI with~~ GLORYS-LR) which differs from the reference in the numerical code and also in the resolvable spatial scales.

The same 3D grid was considered ~~For the observations and~~ for the reference field, the covariance matrices, and to extract the observations at the surface layer or in the vertical profiles at the grid points closest to the mooring locations (Fig. 1b). The horizontal grid spacing was given by~~fields,~~ the native horizontal grid of IBI ~~(~~and GLORYS-HR~~) was used~~ (1/12 º) (Fig. 1b). Thus,~~2). For the covariance matrices, the native grid was used~~ for the computation of the covariance matrices~~ROOI with IBI and GLORYS-HR, while for the ROOI~~ with GLORYS-LR, the data were linearly interpolated to the IBI grid points. The vertical configuration~~resolution~~ was adapted to the levels of the real ADCPs~~a realistic case, emulating ADCP measurements~~ with data every 8 m, ~~meters. The current vertical profiles were set~~ from -12 m to -148 m. Since ~~and~~ the surface layer was set~~HFR currents~~ at -0.5 m, all~~therefore,~~ the used numerical simulation fields were linearly interpolated to this~~the mentioned~~ vertical configuration ~~levels~~ (i.e. -0.5 m, -12 m, -20 m, -28 m, …, -148 m).

2.4 Skill assessment

The skills of the data-reconstruction methods were assessed by means of the root mean square difference (RMSD) between the reconstructed fields (x) and the reference fields (y). The RMSDs were computed at each point of the 3D grid for each study period and for U and V. Thus, for one grid point and a N timesteps (t) period:

$$RMSD = \sqrt{\frac{\sum_{t=1}^{N}(x_t - y_t)^2}{N}}, \quad (7)$$

where x_t and y_t are the reconstructed and reference fields at each timestep, respectively.

The relative RMSD to the root mean square (RMS) current (hereinafter RRMSD) was also considered, since the strength and variability of the current are different at different locations of the study area, and therefore, influence the magnitude of the RMSDs. Therefore, the considered relative value is:

$$RRMSD = \frac{RMSD}{RMS}, \quad (8)$$

where

$$RMS = \sqrt{\frac{\sum_{t=1}^{N}(y_t)^2}{N}}. \quad (9)$$

Since RMSD and RRMSDs were computed for each study period and for each velocity component, hereinafter we use RMSD-U and RRMSD-U as RMSD and RRMSD computed for U and RMSD-V and RRMSD-V as RMSD and RRMSD computed for V. ~~-~~When the RRMSD is equal to 1 at one point for a study period, it means that the RMSD equals the RMS of the studied period at that point.

3 Describing~~Results and discussion~~

~~3.1 Mapping~~ the spatio-temporal variability in the study area~~case~~

In this section, the characteristics of the simulated IBI~~emulated~~ currents ~~in the study area~~ are validated against those found in previous studies based on real HFR and ADCP data (e.g. Rubio et al., 2013, 2019; Solabarrieta et al., 2014). We focus on the comparison of the statistical properties (i.e. spatiotemporal correlations), which are also the basis for the reconstruction methods, and~~analysed~~ in particular, on the~~terms of~~ spatial correlation length scales and temporal cross-correlations (See Appendix A, for a detailed description on the computation of the correlations).~~.~~ The main aim is to provide a previous~~an~~ overview of the ~~emulated~~ currents used to test the ~~3D~~ data-reconstruction methods as ground information, in order to justify the scenarios and to support the discussion on the~~their~~ performances of the data-reconstruction methods. Indeed, the best performances are expected in the areas and periods of higher cross-correlation between currents at different locations and vertical levels.

As shown in Table 2, the spatial ~~The~~ correlation (R) between two variables x_1 and x_2 is defined as follows:

$$R(x_1, x_2) = \frac{E[(x_1-\mu_1)\cdot(x_2-\mu_2)]}{\sqrt{E[(x_1-\mu_1)\cdot(x_1-\mu_1)]\cdot E[(x_2-\mu_2)\cdot(x_2-\mu_2)}}, \quad (10)$$

~~where μ_t is the mean value of x_t, that is, $\mu_t = E[x_t]$. In this study, the correlation was used to estimate the relationships between the emulated horizontal currents in two different ways: by means of spatial relationships, determined by spatial correlation length scales (horizontal and vertical), and by means of temporal relationships, determined by temporal cross-correlations between two different points for a certain period of time. Note that for all the correlations presented here the confidence level considered is 95 %.~~

~~The spatial correlation length scales are the maximum distances between the grid points where the currents can be considered that are related. These scales were calculated for each velocity component, considering meridional and zonal directions for the computation by means of the e-folding method (described in Ha et al., 2007). If we consider one grid, one velocity component and one direction for the computation we can obtain one R value for each fixed distance between the grid points. That is, if for example we consider the zonal direction and the U component, x_1 will be the value of U at each grid point and x_2 will be the value of U at the grid point that is at a fixed distance away (a certain number of grid points in the zonal direction) from the grid point where x_1 is evaluated. Therefore, we will obtain one R value for a fixed distance. Then, R is estimated for all the~~

possible distances, thus obtaining correlation values depending on the distance between the grid points. This operation can be repeated for different time steps through a time period, obtaining a correlation vs distance profile for each time step. All these profiles are then averaged for the time period that interests us, obtaining an averaged correlation vs distance profile. In order to determine the spatial correlation length scale, as explained in Ha et al. (2007), a cut-off point is assumed in the averaged profile where the correlation coefficient decrease to e^{-1} times its original value.

length scales are higher for U than for V, alongIn the water column, U presents higher vertical spatial correlation length scales than V for both moorings. The higher vertical correlation in U was expected buoys (see Table 3) since the profilesboth are located in the Spanish slope, where the zonal slope current prevails. The highest correlation values are observed atdominates the circulation in the area. In addition, these scales are even higher for Matxitxako, which is under a stronger influence of the slope current (with high along-slope spatial correlation) (Rubio et al., 2013; Solabarrieta et al., 2014). TheFor both velocity components, the scales are larger in winter than in summer when the water column is well-mixed and stratified, respectively (Rubio et al., 2013; Rubio et al., 2019).

With regard to surface currents, the horizontal spatial correlation length scales are higher forwhen the along-slope direction of the velocity components when consideringcomponent and the sameconsidered direction for the computation of the correlation (i.e.(zonal or meridional) are the same, being the highest for U, correlation computed (see Table 3). This is due to the slope current that flows in the zonal direction along the Spanish coast, (W-E coast) and for V, correlation computed along thein meridional direction along the French coast). The highest horizontal spatial correlation length scales are observed along the Spanish coast and(N-S coast). Moreover, the scales are slightly larger in winter than in summer. These results are coherent with, when the presence of the along-slope current in the area, which is stronger and more persistent in winter and along the Spanish coastal area (Solabarrieta et al., 2014).

ConcerningRegarding the temporal cross-correlationrelationships, the same patterns shown bytemporal cross-correlation is defined as the spatial correlation of a variable between two different points of a grid for a period of time, that is, the correlation value R between a variable at one point (x_1) and a variable at another point (x_2) throughout the period of time length scales are observed when examiningthat interests us.

For the temporal cross-correlation profiles between the surface and subsurfacethe water column levels at the buoy points, U (Fig. 3)3a and the temporal cross-b) shows higher correlations maps (Figs. 4-5). It is shown that the highestalong the water column in Matxitxako than in Donostia, which agrees with a stronger influence of the slope current at Matxitxako location. For V (Fig. 3c and d) higher correlations are observed for the along-slope in Donostia than in Matxitxako probably due to the stronger signal of this velocity component of the current in winter (with maximum correlationin that area where there is a change of direction on the bathymetry from zonal direction along the Spanish slope to meridional direction along the French slope. As expected, the correlation decreases with depth and it is seasonally modulated in coherence with the water column properties in the area (higher stratification decouples surface from sub-surface processes).

The temporal cross-correlation maps between the ADCP vertical levels at Matxitxako) and that and the surface points of the HFR grid for U (Fig. 4) show that there is a high temporal correlation between Matxitxako and Donostia velocities and in their

~~nearby areas over the Spanish shelf and slope along the whole analysed water column. For both sites it seems that the core of the slope current is well sampled with a stronger signature of such current in Matxitxako. With regard to the seasonality, the correlation is higher and more extended to higher latitudes in winter than in summer, when, as mentioned before, the slope current is stronger and more persistent.~~

~~For V there is a low (almost null) correlation between Matxitxako and Donostia locations (Fig. 5) and along the Spanish shelf and slope. Higher correlations are found in areas closer to the buoys, which extend to the north in the meridional direction. For Matxitxako, this fact is more remarkable in summer than in winter, when the current is not so constrained to the Spanish slope. For Donostia, correlations are high along the French shelf and slope, especially in winter, showing how the slope current follows the bathymetry. The maps show that for both velocity components,~~ the decrease of the correlation with~~in~~ depth is sharper~~stronger~~ in summer than in winter~~, showing the stratified and the mixed water column periods, respectively~~.

It is worth highlighting that the model-based~~emulated~~ spatial correlation length scales and temporal cross-correlations are coherent with those~~the ones~~ obtained from~~using~~ real observations (Rubio et al., 2019; see also supplementary material S1), ~~thus~~ validating ~~further~~ the use of IBI to emulate the study case of the SE-BoB observatory.

4 Results and discussion

4.1~~3.2~~ Data-reconstruction

~~Considering all the analysed depths along the water column (from surface to ~150 m), both study periods and both data-reconstruction methods, satisfactory reconstructions are obtained. These reconstructions provide mean RMSDs for each depth (Figs.~~ The results, in terms of RMSDs and RRMSDs are summarized in Table 3. ~~10-11) ranging from 0.55 (0.7) cm s^{-1} to 10.94 (9.58) cm s^{-1} for the whole (reduced) grid and mean RRMSDs ranging from 0.07 (0.12) to 3.47 (1.31) with typical values around 1 or less, that is, with reconstructed field errors around the RMS or less at each point. Although, in general, the RRMDs are increased with depth (thus, showing a worse performance), mean RMSDs lower than 10.94 cm s^{-1} are obtained at ~150 m. The results obtained in this study are summarized in Table 4, where the spatial mean RMSDs and RRMSDs are shown for three different depths, for both study periods, for both data-reconstruction methods (the ROOI with GLORYS-LR) and for the whole and reduced grids.~~

It is observed that, in general, the RMSDs and the RRMSDs are affected by the spatial and temporal variability of the slope current regime~~. for the study area described in Sect. 3.1.~~ The mean RMSDs are higher in winter than in summer due to ~~because currents are~~ more intense currents in that period. However~~, however~~, the RMSs are also higher ~~in that period~~ and in relative terms the reconstructions show better results in winter (lower mean RRMSDs). This dependence of the results on the current regime can be also observed if we compare the reduced and the entire~~whole~~ grid cases. For the reduced grid case, that covers an area of intense zonal slope currents, highest mean RMSDs and lowest mean RRMSDs are obtained for U. Since V is much weaker for this grid, it provides the lowest mean RMSDs. Nevertheless~~, nevertheless~~, the expected increase in the mean RRMSDs is not so clear compared to the entire~~whole~~ grid case due to lower RMSs.

Regarding the comparison between data-reconstruction~~both~~ methods, for the entire~~whole~~ grid case, the mean RRMSD-Us are remarkably higher for the DCT-PLS, whereas the RRMSD-V provides similar results for both. Conversely~~On the other hand~~, for the reduced grid case, the results for the RRMSD-U for the DCT-PLS are better. This shows~~, showing~~ that the DCT-PLS~~this method~~ performs better in well sampled areas whereas~~while~~ the ROOI performs well also out~~better than the DCT-PLS in the rest~~ of these~~the~~ areas. ~~(although it also performs well in the former area).~~

All these results, in addition to more specific analyses, are shown below in terms of RRMSDs by means of maps (Figs. 6-9) and horizontal mean values' profiles~~graphs~~ along the water column (Figs. 10-11). The results of the RMSDs are shown in supplementary material S4. For the ROOI RRMSD maps, the results with the spatial covariances from GLORYS-LR are the ones presented in Figs. 6-7 because those are the ones that most challenge the method. In fact, for the ROOI with GLORYS-HR the RRMSDs are even lower (see supplementary material S2), being~~however~~ the main conclusions ~~are~~ very similar.

For the ROOI, the RRMSD spatial distribution is more uniform in summer (Fig. 6) than in winter (Fig. 7) due to the more variable summer current regime. The Spanish slope area shows the lowest RRMSD-Us due to the strong signal of the along-slope current, with lower values in winter than in summer. This suggests~~, suggesting~~ that the reconstructed fields are more accurate in well sampled areas and that U is well resolved in the numerical simulations used for the definition of the spatial covariances. For the RRMSD-V, the French slope and part of its platform show the lowest values in winter, indicating that the slope current is well reconstructed for that period. Since the density of the observation is much higher at the surface, it is expected the method to perform better in the upper layers, in fact, it is observed that the RRMSDs increase with depth. This increase is sharper in~~more remarkable for~~ summer than in~~for~~ winter, probably due to higher vertical shear in the currents due to the stratification conditions. It is shown that for the ROOI with GLORYS-LR, the RRMSDs are below 1.25, that is, the RMSD is below 1.25 times the RMS at each point, except for some concrete areas.

With regard to the DCT-PLS, RRMSD maps (Figs. 8-9) show ~~), it is observed that the values are~~ the lowest values near to the surface and the moorings~~buoys~~ locations, showing that this method's skills are better ~~adjusted~~ in well sampled areas. The~~For both velocity components, the~~ RRMSDs are lower in winter (Fig. 9) than in ~~9), being characterized by stronger and persistent currents compared to the~~ summer ~~regime~~ (Fig. 8). For the RRMSD-U, the Spanish slope area shows the lowest values for both periods, whereas low RRMSD-Vs are observed over the French slope in winter, showing that this method is also able to reconstruct the slope current. Overall, RRMSDs increase with depth~~;~~, nevertheless, ~~for RRMSD-V~~ in summer~~,~~ the ~~RRMSD-V~~values are higher for -52 m (Fig. 8d) than for -100 m (Fig. 8f). This could be related to a stronger~~the water depths where the~~ vertical shear related~~of the currents is expected~~ to ~~be the highest due to the presence of~~ the seasonal thermocline, which in this period is located between -30 m and -50 m. For the DCT-PLS, the RRMSDs are not as smooth as for the ROOI, with RMSDs near (off) the observation areas lower (higher) than half (~~the RMS at each point and values out of those areas higher than~~ twice) the RMS at each point.

Thus, for both methods lower RRMSDs are observed in winter than in summer~~, and~~ along the slope for the along-slope component of the velocity and close to the surface.~~; with RRMSDs increasing with depth.~~ While, the DCT-PLS is more effective at well sampled areas, the ROOI performs better at~~for~~ the rest of the areas. In general, the best performances are

located in the well-sampled areas~~areas where correlations between velocities in the ADCP locations and the rest of the grid locations are high~~ (Figs. 3-5), showing that the~~this~~ a-priori analysis, ~~(~~shown in Sect. 3~~.1)~~ can provide an approximate idea about the areas where the ~~data~~ reconstructions could, in principle, perform better.

It is observed that the results for the DCT-PLS worsen quickly as we get away from the observation points. Considering the -52 m depth layer, we observe that RRMSD values obtained with the DCT-PLS method increase from 0 to 0.25 at ~31 km (6.3 km) for the U(V) component in the zonal (meridional) direction.

A further~~The~~ analysis of the spatial mean of the RRMSDs with depth (Figs. 10-11) is performed~~aimed~~ to evaluate the~~compare both data-reconstruction~~ methods' skills, regardless of the spatial variability shown in previous figures. Note that the ROOI with both IBI and GLORYS- LR and HR are shown in this analysis. The ~~, and that the~~ same grid points were considered for both data-reconstruction ~~all the~~ methods, in the entire ~~and products. The whole~~ grid and the reduced grid (see Fig. 1b) ~~were considered~~ in order to explore the sensitivity of the results to the choice of different areas.

For the entire~~whole~~ grid case (Fig. 10), the ROOI with ~~IBI and GLORYS-HR performs better for both velocity components, whereas, the ROOI with~~ GLORYS-LR provides similar results as the DCT-PLS for V (Fig. 10b and d), whereas~~) and~~ it provides much better results for U (Fig. 10a and c). On the other hand, the ROOI with IBI and GLORYS-HR performs better for both velocity components. In addition, as it could be noticed in Table 3~~4~~ and along Figs. 6-9, the mean RRMSDs show RMSDs around ~~1~~ or less than one times the RMS at each point, except for U for the DCT-PLS.

In the reduced grid case (Fig. 11), the lowest mean RRMSD-Us are observed for the DCT-PLS, performing~~working~~ significantly better than the ROOI. In general, the~~The~~ mean RMSDs are around ~~0.75~~ or less than 0.75 times the RMS at each point, with values around ~~0.5~~ or less than 0.5 times the RMS for the DCT-PLS. This provides~~, providing~~ quite a satisfactory reconstruction of the along-slope velocity component in the Spanish slope area. Thus, if ~~we consider~~ the whole water column is considered, the ROOI provides again smaller RRMSDs than the DCT-PLS for the entire~~whole~~ grid case, whereas, the DCT-PLS provides better results in well sampled areas.

With regard to the seasonal analysis lower RRMSDs are~~, as~~ observed in winter~~the maps~~ (Figs. ~~6-9), overall, for both data-reconstruction methods and for both velocity components, Figs.~~ 10-11). The only exception is ~~show lower RRMSDs in winter than in summer, except for~~ the RRMSD-U in the entire~~whole~~ grid case for the DCT-PLS (Figs. 10 a and c) due to~~). This exception was caused by~~ the high~~big~~ RRMSDs over the French shelf and slope for that period (see supplementary material S3), since this method expands the zonal component to that area of meridional regime.

Considering all the analysed depths and study periods, satisfactory reconstructions are obtained by both methods~~3.3 Sensitivity test: increased number of ADCPs~~

. These reconstructions provide mean RMSDs for each depth (Figs. 10-11) ranging from 0.55 (0.7) cm s^{-1} to 10.94 (9.58) cm s^{-1} for the entire (reduced) grid and mean RRMSDs ranging from 0.07 (0.12) to 3.47 (1.31) with typical values around 1 or less, that is, with reconstructed field errors around the RMS or less at each point. In general, the RRMDs are increased with depth and thus RMSDs up to 10.94 cm s^{-1} are obtained at -150 m.

4.2 Sensitivity test: increased number of ADCPs

An analysis with ~~observations of ADCPs in~~ two additional ADCPs~~locations~~ was carried out, in order evaluate the sensitivity of the data-reconstruction methods to an increased number of observations. ~~with higher geographical coverage.~~ The two extra ADCPs were located over the French slope, since this could be a strategic area to monitor the winter slope current downstream the Capbreton canyon.

Only the winter period is shown, when the slope current is the strongest and the effects of the new scenario are more noticeable (note that we show~~. We selected~~ here ~~only~~ the results obtained for the -52 m layer, due to its representativeness of the entire ~~changes between the 2-buoy and the 4-buoy scenario for all the~~ water column). ~~levels analysed before.~~ The performance of the data-reconstruction methods for this configuration is assessed~~shown~~ subtracting the RRMSD maps of the 2-mooring~~buoy~~ case to the 4-mooring~~buoy~~ case. Therefore, the negative (positive) values in Fig. 12 show that the RRMSD is lower (higher) for the 4-mooring~~buoy~~ configuration;~~,~~ thus, showing a better (worse) performance. In general, in this new scenario ~~improves~~ the performance of both data-reconstruction methods improves, with smoother changes for the ROOI, since it already uses historical information of the covariances in the whole study area~~, including the locations of the extra ADCPs.~~

For U, the addition of two extra ADCP~~ADPC~~ profiles does not affect the Spanish slope area where there are already two moorings that capture the slope current. In the rest of the grid, for the DCT-PLS (Fig. 12b),~~,~~ the performance of the reconstruction is remarkably improved; whereas, for the ROOI (Fig. 12a),~~,~~ although in general the reconstruction is improved, there are some specific areas where the RRMSD-Us are slightly increased.

For V, the results improve along the French slope, which are more remarkable for the DCT-PLS (Fig. 12d).~~.~~ However, for this method, the RRMSD-Vs are increased in the areas close to that slope, probably due to the spread of the information from~~signal of~~ the slope observations to those nearby areas which are not affected by the slope current regime.

~~5All in all, the reconstructions of the along-slope component are improved with the additional observations.~~

~~4~~ Summary and Conclusions.

In this paper we investigated the feasibility~~combination~~ of combining data ~~obtained~~ from multiplatform observing systems to reconstruct ~~the~~ 3D velocity fields~~field~~ in the SE-BoB~~a shelf-slope region~~ by means of two data-reconstruction methods. More precisely, we assessed the performance of such methods in ~~investigated~~ the case of combining surface current data (as the ones provided by a long-range ~~velocities obtained from a~~ HFR system) and current vertical~~velocity~~ profiles (as the ones provided~~measured~~ by two moorings equipped with ADCPs), in an emulated scenario based on an existing observatory (being also ~~, which is~~ a typical configuration that can be found in other ~~among the existing~~ coastal areas).~~observatories.~~ The performances of the methods~~reconstructions~~ were assessed through a classical approach conceptually similar to OSSEs, where a realistic~~controlled reality experiment in which observations were extracted from a numerical~~ simulation was regarded as the "true" ocean. This assessment approach allowed ~~and~~ the comprehensive evaluation~~results compared to the original simulated fields.~~

~~A preliminary spatial correlation length scale analysis and a temporal cross-correlation analysis provided a first guess~~ of the selected methods as a first step towards their application to real data in the study area. Besides, it provides a best-practice methodology for ~~areas where~~ the evaluation of the challenges and limitations of this kind of methods in a broader way, prior to their applications to real data in other study cases. An interesting further step, out of the scope of the present paper, would be to evaluate the robustness of the reconstruction methods for different observational errors.

~~reconstructions could perform better.~~ We obtained satisfactory reconstruction results with spatial mean RMSDs typically ranging between 0.55–7~~10.94~~ cm s^{-1}, for the first 150 m depth, with mean~~which represents a~~ relative errors~~error~~ of 0.07–1.2~~3.47~~ times the RMS current at each point for most of~~. In addition,~~ the cases. The~~results show that the~~ main feature of the region, the slope current, was~~is~~ well reconstructed by both methods, and significantly improved when the information~~. The results have also shown that the addition~~ of two additional moorings were used for the ~~can improve significantly the results of the~~ reconstruction.

Regarding the data-reconstruction methods, each one has its pros and cons. The DCT-PLS is only fed with the observations with no extra information about the study area, so its configuration is simpler. It performs well in well sampled areas, but its quality is quickly degraded elsewhere. On the other hand, the ROOI is a robust data-reconstruction method that uses additional historical information~~ of the study area~~, and thus provides better results in under~~areas which are not~~ sampled areas. The shortcoming of this method is that it needs accurate historical information of the study area. This is typically obtained from a realistic numerical simulation of the region although it does not need to be contemporary to the observational period (i.e. from a hindcast simulation)~~.~~ Also, the method requires more tuning, so its implementation demands a careful testing of the parameters.

The tested~~These data reconstruction~~ methods have proven to be reliable, showing that it would be feasible to use them to reconstruct 3D current fields in the study area. In addition, they also~~ and~~ could be used in a wide range of applications~~. For instance,~~ due to their low computational cost. As, for instance,~~ they could be used~~ to obtain new operational products, combining data from different sources and complementary spatial coverage in near real time. Moreover, through OSSE and ~~Observing System Simulation Experiments and~~ Observing System Experiments (OSEs~~OSSE and OSE~~) an optimization of existing observing networks can be proposed, providing a potential decision-making tool~~ for taking decisions~~ for future planning of coastal observatories or to set-up optimal operational data assimilation strategies. The use of these methods can be an alternative to data assimilation approaches (more expensive computationally and more complex to set-up) as far as they do not require to run a numerical model. This is especially appealing for marine rapid environmental assessment (MREA). The 3D reconstructed velocity fields can also be used~~Additionally, the 3D velocity reconstructions might have applications for coastal risk assessment or~~ for model validation, as well as for broadening the utility of coastal observing systems to biological, geochemical and environmental issues.

Appendix A

The correlation (R) between two variables x_1 and x_2 is defined as follows:

$$R(x_1, x_2) = \frac{E[(x_1-\mu_1)\cdot(x_2-\mu_2)]}{\sqrt{E[(x_1-\mu_1)\cdot(x_1-\mu_1)]\cdot E[(x_2-\mu_2)\cdot(x_2-\mu_2)]}}, \quad (10)$$

where μ_i is the mean value of x_i, that is, $\mu_i = E[x_i]$. In this study, the correlation was used to estimate the relationships between the emulated horizontal currents in two different ways: by means of spatial relationships, determined by spatial correlation length scales (horizontal and vertical), and by means of temporal relationships, determined by temporal cross-correlations between two different points for a certain period of time. Note that for all the correlations presented here the confidence level considered is 95 %.

The spatial correlation length scales are the maximum distances between the grid points where the currents can be considered that are related. These scales were calculated for each velocity component, considering meridional and zonal directions for the computation by means of the e-folding method (described in Ha et al., 2007). If we consider one grid, one velocity component and one direction for the computation we can obtain one R value for each fixed distance between the grid points. That is, if we consider the zonal direction and the U component, x_1 will be the value of U at each grid point and x_2 will be the value of U at the grid point that is at a fixed distance away (a certain number of grid points in the zonal direction) from the grid point where x_1 is evaluated. Therefore, we will obtain one R value for a fixed distance. Then, R is estimated for all the possible distances, thus obtaining correlation values depending on the distance between the grid points. This operation can be repeated for different time steps through a time period, obtaining a correlation vs distance profile for each time step. All these profiles are then averaged for the time period that interests us, obtaining an averaged correlation vs distance profile. In order to determine the spatial correlation length scale, as explained in Ha et al. (2007), a cut-off point is assumed in the averaged profile where the correlation coefficient decrease to e^{-1} times its original value.

Regarding the temporal relationships, the temporal cross-correlation is defined as the correlation of a variable (or two different variables) between two different points of a grid for a period of time, that is, the correlation value R between a variable at one point (x_1) and a variable at another point (x_2) throughout the period of time analysed.

Data availability

The IBI_REANALYSIS_PHYS_005_002 product is available on the CMEMS website (http://marine.copernicus.eu/services-portfolio/access-to-products/?option=com_csw&view=details&product_id=IBI_REANALYSIS_PHYS_005_002).

The GLOBAL_REANALYSIS_PHY_001_025 product is available on the CMEMS website (http://marine.copernicus.eu/services-portfolio/access-to-products/?option=com_csw&view=details&product_id=GLOBAL_REANALYSIS_PHY_001_025).

The GLOBAL_REANALYSIS_PHY_001_030 product is available on the CMEMS website (http://marine.copernicus.eu/services-portfolio/access-to-products/?option=com_csw&view=details&product_id=GLOBAL_REANALYSIS_PHY_001_030).

Author Contributions

IMN, EF, GJ, MB, AG, AC, AR: contribution to the main structure and contents. In addition, IMN produced the figures and EF, GJ provided the software, the tools and gave advice for the reconstruction with the DCT-PLS and ROOI methods, respectively.

Competing interests

The authors declare that they have no conflict of interest.

Acknowledgments

This study has been supported by the JERICO-NEXT project, funded by the European Union's Horizon 2020 research and innovation programme under grant agreement No 654410. This study has been also undertaken with the financial support of the Department of Environment, Regional Planning, Agriculture and Fisheries of the Basque Government (Marco Program). I. Manso was supported by a PhD fellowship from also the Department of Environment, Regional Planning, Agriculture and Fisheries of the Basque Government. This study has been conducted using E.U. Copernicus Marine Service Information. This is contribution number XXX, of the Marine Research Division of AZTI-Tecnalia.

References

Barrick, D.: First-order theory and analysis of MF/HF/VHF scatter from the sea, IEEE T. Antenn. Propag., 20, 2-10, https://doi.org/10.1109/TAP.1972.1140123, 1972.

Broche, P., Forget, P., De Maistre, J., Devenon~~Alvera-Azcárate, A., Barth, A., Rixen, M., and Beckers, J. M.: Reconstruction of incomplete oceanographic data sets using empirical orthogonal functions: application to the Adriatic Sea surface temperature, Ocean Model., 9, 325-346, 10.1016/j.ocemod.2004.08.001, 2005.~~

~~Alvera-Azcárate, A., Barth, A., Beckers~~, J~~. M~~., and Crochet, M.: VHF radar for ocean surface current~~Weisberg, R. H.: Multivariate reconstruction of missing data in sea surface temperature, chlorophyll,~~ and ~~wind satellite fields, J. Geophys.~~ sea state remote sensing, Radio Sci., 22, 69-75~~Res., 112, C03008~~, https://doi.org/10.1029/RS022i001p00069, 1987~~2006JC003660, 2007.~~

Barth, A., Beckers, J.-M., Troupin, C., Alvera-Azcárate, A., and Vandenbulcke, L.: divand-1.0: n-dimensional variational data analysis for ocean observations, Geosci. Model Dev., 7, 225-241, doi:10.5194/gmd-7-225-2014, 2014.

Beckers, J. M., and Rixen, M.: EOF calculations and data filling from incomplete oceanographic datasets, J. Atmos. Ocean. Tech., 20(12), 1839-1856, https://doi.org/10.1175/1520-0426(2003)020%3C1839:ECADFF%3E2.0.CO;2, 2003.

Chapman, R., Shay, L. K., Graber, H. C., Edson, J., Karachintsev, A., Trump, C., and Ross, D.: On the accuracy of HF radar surface current measurements: Intercomparisons with ship-based sensors, J. Geophys. Res.-Oceans, 102, 18737-18748, https://doi.org/10.1029/97JC00049, 1997.

Church, J. A., and White, N. J.: A 20th century acceleration in global sea-level rise, Geophys. Res. Lett., 33, L01602, https://doi.org/10.1029/2005GL024826, 2006.

Cianelli, D., Falco, P., Iermano, I., Mozzillo, P., Uttieri, M., Buonocore, B., ZambardinoEsnaola, G., Sáenz, J., Zorita, E., Fontán, A., Valencia, V., and Zambianchi, E.: Inshore/offshore water exchangeLazure, P.: Daily scale wintertime sea surface temperature and IPC-Navidad variability in the Gulfsouthern Bay of Naples, J. Marine Syst., 145, 37-52Biscay from 1981 to 2010, Ocean Sci., 9, 655-679, https://doi.org/10.1016/j.jmarsys.2015.01.002, 2015.

Davies, A. M.: On determining current profiles in oscillatory flows, Appl. Math. Model., 9, 419-428, https://doi.org/10.1016/0307-904X(85)90107-6, 1985a.

Davies, A. M.: On determining the profile of steady wind-induced currents, Appl. Math. Model., 5194/os 9, 409-418, https://doi.org/10.1016/0307-904X(85)90106-4, 1985b.

Davies, A. M.: Three dimensional modal model of wind induced flow in a sea region, Prog. Oceanogr., 15, 71-128, https://doi.org/10.1016/0079-6611(85)90032-1, 1985c.

De Valk, C.F.: Estimation of 3-D current fields near the Rhine outflow from HF radar surface current data, Coast. Eng., 37, 487-511, https://doi.org/10.1016/S0378-3839(99)00040-X, 1999 655-2013, 2013.

Fredj, E., Roarty, H., Kohut, J., Smith, M., and Glenn, S.: Gap filling of the coastal ocean surface currents from HFR data: Application to the Mid-Atlantic Bight HFR Network, J. Atmos. Ocean. Tech., 33, 1097-1111, https://doi.org/10.1175/JTECH-D-15-0056.1, 2016.

Frouin, R., Fiúza, A. F., Ambar, I., and Boyd, T. J.: Observations of a poleward surface current off the coasts of Portugal and Spain during winter, J. Geophys. Res.-Oceans, 95, 679-691, https://doi.org/10.1029/JC095iC01p00679, 1990.

Fujii, S., Heron, M. L., Kim, K., Lai, J.-W., Lee, S.-H., Wu, X., Wu, X., Wyatt, L. R., and Yang, W.-C.: An overview of developments and applications of oceanographic radar networks in Asia and Oceania countries, Ocean Sci. J., 48, 69-97, http://dx.doi.org/10.1007/s12601-013-0007-0, 2013.

Gangopadhyay, A., Shen, C. Y., Marmorino, G. O., Mied, R. P., and Lindemann, G. J.: An extended velocity projection method for estimating the subsurface current and density structure for coastal plume regions: An application to the Chesapeake Bay outflow plume, Cont. ~~Gandin, L. S.: Objective Analysis of Meteorological Fields. Israel Program for Scientific Translations, Jerusalem, Israel: QJR Meteorolog. Soc, 1965.~~
Shelf Res., 25, 1303-1319, https://doi.org/10.1016/j.csr.2005.03.002, 2005.

Garcia, D.: Robust smoothing of gridded data in one and higher dimensions with missing values, Comput. Stat. Data An., 54, 1167-1178, https://doi.org/10.1016/j.csda.2009.09.020, 2010.

Ha, K.-J., Jeon, E.-H., and Oh, H.-M.: Spatial and temporal characteristics of precipitation using an extensive network of ground gauge in the Korean Peninsula, Atmos. Res., 86, 330-339, https://doi.org/10.1016/j.atmosres.2007.07.002, 2007.

Haynes, R., and Barton, E. D.: A poleward flow along the Atlantic coast of the Iberian Peninsula, J. Geophys. Res.-Oceans, 95, 11425-11441, https://doi.org/10.1029/JC095iC07p11425, 1990.

Ivonin, D. V., Broche, P., Devenon, J.~~Hernández-Carrasco, I., Solabarrieta,~~ L., ~~Rubio, A., Esnaola, G., Reyes, E.,~~ and Shrira, V. I.: Validation~~Orfila, A.: Impact~~ of HF radar probing of the vertical shear of surface currents by acoustic Doppler current profiler measurements, J. ~~gap filling methodologies on the Lagrangian assessment of coastal dynamics, Ocean Sci., 14, 827-847~~Geophys. Res.-Oceans, 109, https://doi.org/10.1029/2003JC002025, 2004~~5194/os-14-827-2018, 2018~~.

Jordà, G., Sánchez-Román, A., and Gomis, D.: Reconstruction of transports through the Strait of Gibraltar from limited observations, Clim. Dynam., 48, 851-865, https://doi.org/10.1007/s00382-016-3113-8, 2016.

Kaplan, ~~D. M., and Lekien, F.: Spatial interpolation and filtering of surface current data based on open-boundary modal analysis, J. Geophys. Res. Oceans, 112, C12007, https://doi.org/10.1029/2006JC003984, 2007.~~

~~Kaplan,~~ A., Kushnir, Y., Cane, M. A., and Blumenthal, M. B.: Reduced space optimal analysis for historical data sets: 136 years of Atlantic sea surface temperatures, J. Geophys. Res.-Oceans, 102, 27835-27860, https://doi.org/10.1029/97JC01734, 1997.

Kaplan, A., Kushnir, Y., and Cane, M. A.: Reduced space optimal interpolation of historical marine sea level pressure: 1854–1992, J. Climate, 13, 2987-3002, https://doi.org/10.1175/1520-0442(2000)013%3C2987:RSOIOH%3E2.0.CO;2, 2000.

~~Kohonen, T.: Self-organized formation of topologically correct feature maps, Biol. Cybern., 43, 59-69, https://doi.org/10.1007/BF00337288, 1982.~~

~~Kohonen, T.: Self-Organizing Maps, 2nd edn., Springer, Heidelberg, Germany, 1997.~~

Le Cann, B., and Serpette, A.: Intense warm and saline upper ocean inflow in the southern Bay of Biscay in autumn–winter 2006–2007, Cont. Shelf Res., 29, 1014-1025, https://doi.org/10.1016/j.csr.2008.11.015, 2009.

Marmorino, G., Shen, C., Evans, T., Lindemann, G., Hallock, Z., and Shay, L. K.: Use of 'velocity projection'to estimate the variation of sea-surface height from HF Doppler radar current measurements, Cont. Shelf Res., 24, 353-374, https://doi.org/10.1016/j.csr.2003.10.011, 2004.

O'Donncha, F., Hartnett, M., Nash, S., Ren, L., and Ragnoli, E.: Characterizing observed circulation patterns within a bay using HF radar and numerical model simulations J. Marine Syst., 142, 96-110, https://doi.org/10.1016/j.jmarsys.2014.10.004, 2015.

Paduan, J. D., and Graber, H. C.: Introduction to high-frequency radar: reality and myth, Oceanography, 10, 36-39, https://doi.org/10.5670/oceanog.1997.18, 1997.

Paduan, J. D., and Washburn, L.: High-frequency radar observations of ocean surface currents, Annu. Rev. Mar. Sci., 5, 115-136, https://doi.org/10.1146/annurev-marine-121211-172315, 2013.

Peliz, Á., Dubert, J., Haidvogel, D. B., and Le Cann, B.: Generation and unstable evolution of a density-driven eastern poleward current: The Iberian Poleward Current, J. Geophys. Res.-Oceans, 108(C8), 3268, https://doi.org/10.1029/2002JC001443, 2003.

Pingree, R., and Le Cann, B.: Structure, strength and seasonality of the slope currents in the Bay of Biscay region, J. Mar. Biol. Assoc. UK, 70, 857-885, https://doi.org/10.1017/S0025315400059117, 1990.

Pingree, R., and Le Cann, B.: Three anticyclonic Slope Water Oceanic eDDIES (SWODDIES) in the southern Bay of Biscay in 1990, Deep-Sea Res., 39, 1147-1175, https://doi.org/10.1016/0198-0149(92)90062-X, 1992a.

Pingree, R., and Le Cann, B.: Anticyclonic eddy X91 in the southern Bay of Biscay, May 1991 to February 1992, J. Geophys. Res.-Oceans, 97, 14353-14367, https://doi.org/10.1029/92JC01181, 1992b.

Prandle, D.: The vertical structure of tidal currents, Geophys. Astro. Fluid, 22, 29-49, https://doi.org/10.1080/03091928208221735, 1982.

Prandle, D.: The fine-structure of nearshore tidal and residual circulations revealed by HF radar surface current measurements, J. Phys. Oceanogr., 17, 231-245, https://doi.org/10.1175/1520-0485(1987)017%3C0231:TFSONT%3E2.0.CO;2, 1987.

Prandle, D.: A new view of near-shore dynamics based on observations from HF radar, Prog. Oceanogr., 27, 403-438, https://doi.org/10.1016/0079-6611(91)90030-P, 1991.

Ren, L., Nash, S., and Hartnett, M.: Observation and modeling of tide-and wind-induced surface currents in Galway Bay, Water Science and Engineering, 8, 345-352, https://doi.org/10.1016/j.wse.2015.12.001, 2015.

Roarty, H., Cook, T., Hazard, L., George, D., Harlan, J., Cosoli, S., Wyatt, L., Fanjul, E., Terrill, E., Otero, M., Largier, J., Glenn, S., Ebuchi, N., Whitehouse, B., Bartlett, K., Mader, J., Rubio, A., Corgnati, L., Mantovani, C., Griffa, A., Reyes, E., Lorente, P., Flores-Vidal, X., Saavedra-Matta, K., Rogowski, P., Prukpitikul, S., Lee, S.-H., Lai, J.-W., Guerin, C.-A., Sanchez, J., Hansen, B., and Grilli, S.: The Global High Frequency Radar Network, Frontiers in Marine Science, 6, 164, https://doi.org/10.3389/fmars.2019.00164, 2019.

Rubio, A., Fontán, A., Lazure, P., González, M., Valencia, V., Ferrer, L., Mader, J., and Hernández, C.: Seasonal to tidal variability of currents and temperature in waters of the continental slope, southeastern Bay of Biscay, J. Marine Syst., 109, S121-S133, https://doi.org/10.1016/j.jmarsys.2012.01.004, 2013.

Rubio, A., Mader, J., Corgnati, L., Mantovani, C., Griffa, A., Novellino, A., Quentin, C., Wyatt, L., Schulz-Stellenfleth, J., and Horstmann, J.: HF radar activity in European coastal seas: next steps toward a pan-European HF radar network, Frontiers in Marine Science, 4, 8, https://doi.org/10.3389/fmars.2017.00008, 2017.

Rubio, A., Manso-Narvarte, I., Caballero, A., Corgnati, L., Mantovani, C., Reyes, E., Griffa, A., and Mader, J.: The seasonal intensification of the slope Iberian Poleward Current, in: Copernicus Marine Service Ocean State Report, J. Oper. Oceanogr., Issue 3, 13-18, doi: 10.1080/1755876X.2019.1633075, 2019.

Shen, C. Y., and Evans, T. E.: Dynamically constrained projection for subsurface current velocity, J. Geophys. Res.-Oceans, 107, 24-21-24-14, https://doi.org/10.1029/2001JC001036, 2002.

Shen, C. Y., and Evans, T. E.: Surface-to-subsurface velocity projection for shallow water currents, J. Geophys. Res.-Oceans, 106, 6973-6984, https://doi.org/10.1029/2000JC000267, 2001.

Shrira, V. I., Ivonin, D. V., Broche, P., and de Maistre, J. C.: On remote sensing of vertical shear of ocean surface currents by means of a Single-frequency VHF radar, Geophys. Res. Lett., 28, 3955-3958, https://doi.org/10.1029/2001GL013387, 2001.
~~Sasaki, Y.: Some basic formalisms in numerical variational analysis, Mon. Weather Rev., 98, 875-883, 1970.~~

Solabarrieta, L., Rubio, A., Castanedo, S., Medina, R., Charria, G., and Hernández, C.: Surface water circulation patterns in the southeastern Bay of Biscay: new evidences from HF radar data, Cont. Shelf Res., 74, 60-76, https://doi.org/10.1016/j.csr.2013.11.022, 2014.

Sotillo, M., Cailleau, S., Lorente, P., Levier, B., Aznar, R., Reffray, G., Amo-Baladrón, A., Chanut, J., Benkiran, M., and Alvarez-Fanjul, E.: The MyOcean IBI Ocean Forecast and Reanalysis Systems: operational products and roadmap to the future Copernicus Service, J. Oper. Oceanogr., 8, 63-79, https://doi.org/10.1080/1755876X.2015.1014663, 2015.

Stewart, R. H~~Taillandier, V., Griffa, A.~~, and Joy, J. W.: HF radio measurements~~Molcard, A.: A variational approach for the reconstruction~~ of surface currents, Deep-Sea Res., 21, 1039-1049, ~~regional scale Eulerian velocity fields from Lagrangian data, Ocean Model., 13, 1-24,~~ https://doi.org/10.1016/0011-7471(74)90066-7, 1974~~j.ocemod.2005.09.002, 2006~~.

Teague, C. C., Vesecky, J. F., and Hallock, Z. R.: A comparison of multifrequency HF radar and ADCP measurements of near-surface currents during COPE-3, IEEE J. Oceanic Eng., 26, 399-405, https://doi.org/10.1109/48.946513, 2001.
~~Wahba, G., and Wendelberger, J.: Some new mathematical methods for variational objective analysis using splines and cross validation, Mon. Weather Rev., 108, 1122-1143, https://doi.org/10.1175/1520-0493(1980)108%3C1122:SNMMFV%3E2.0.CO;2, 1980.~~

Wyatt, L.: High frequency radar applications in coastal monitoring, planning and engineering, Australian Journal of Civil Engineering, 12, 1-15, 2014.

~~Yaremchuk, M., and Sentchev, A.: Mapping radar-derived sea surface currents with a variational method, Cont. Shelf Res., 29, 1711-1722, https://doi.org/10.1016/j.csr.2009.05.016, 2009.~~

Table 1. List of some data gap-filling/reconstruction methods applied to oceanographic data sets.

Name of the method	Reference
Open-boundary Modal Analysis (OMA)	Kaplan and Lekien, 2007
Data Interpolating Empirical Orthogonal Functions (DINEOF)	Beckers and Rixen, 2003 and Alvera-Azcárate et al., 2005
Self-Organizing Maps (SOM)	Kohonen, 1982, 1997
Variational Analysis (VA)	Sasaki, 1970 and Wahba and Wendelberger, 1980
Optimal Interpolation (OI)	Gandin, 1965
Discrete Cosine Transform Penalized Least Square (DCT-PLS)	García, 2010
Reduced Order Optimal Interpolation (ROOI)	Kaplan et al., 1997

~~**Table 2.**~~ Details of the ~~three~~ numerical simulations used in this study.

	IBI	GLORYS-LR	GLORYS-HR
Product identifier	IBI_REANALYSIS_PHYS_005_002	GLOBAL_REANALYSIS_PHY_001_025	GLOBAL_REANALYSIS_PHY_001_030
Regional / Global	Regional	Global	Global
Spatial resolution	0.083º x 0.083º	0.25º x 0.25º	0.083º x 0.083º
Temporal resolution	Daily	Daily	Daily
Model	NEMO v3.6	NEMO v3.1	NEMO v3.1
Data assimilation	In-Situ TS Profiles Sea Level SST	Sea Ice Concentration and/or Thickness In-Situ TS Profiles Sea Level SST	Sea Ice Concentration and/or Thickness In-Situ TS Profiles Sea Level SST
Atmospheric forcing	ECMWF ERA-interim	ECMWF ERA-interim	ECMWF ERA-interim
Bathymetry	GEBCO_08 + different local Databases	ETOPO1 for deep ocean and GEBCO8 on coast and continental shelf	ETOPO1 for deep ocean and GEBCO8 on coast and continental shelf
Initial conditions	January 1992: T, S, velocity components and sea surface height from GLORYS2V4	December 1991: T, S regressed from EN4	December 1991: T, S regressed from EN.4.2.0
Open boundary data	Data from daily outputs from the CMEMS GLOBAL reanalysis eddy resolving system.	…	…
Application in this study	Observations, reference fields, the covariance matrix for the ROOI	The covariance matrix for the ROOI	The covariance matrix for the ROOI
For a more detailed description:	http://cmems-resources.cls.fr/documents/PUM/CMEMS-IBI-PUM-005-002.pdf http://resources.marine.copernicus.eu/documents/QUID/CMEMS-IBI-QUID-005-002.pdf	http://cmems-resources.cls.fr/documents/PUM/CMEMS-GLO-PUM-001-025.pdf http://resources.marine.copernicus.eu/documents/QUID/CMEMS-GLO-QUID-001-025.pdf	http://cmems-resources.cls.fr/documents/PUM/CMEMS-GLO-PUM-001-030.pdf http://resources.marine.copernicus.eu/documents/QUID/CMEMS-GLO-QUID-001-030.pdf

Table 23. Seasonal spatial correlation length scales for the emulated current velocity components U and V in the study area, for the summer and winter periods and in zonal and meridional directions. Note that the surface horizontal scales are shown in kilometres and that the vertical scales in depth at Matxitxako and Donostia mooringbuoy points are shown in meters.

Current component	Surface (km)				Depth (m)			
	Summer		Winter		Summer		Winter	
	Zonal direction	Meridional direction	Zonal direction	Meridional direction	Matxitxako mooringbuoy	Donostia mooringbuoy	Matxitxako mooringbuoy	Donostia mooringbuoy
U	78	15	79	16	24	23	88	43
V	11	60	12	73	19	15	30	36

Table 34. Summary of the results of the reconstructions with ROOI (with GLORYS-LR) and DCT-PLS in terms of spatial mean RMSDs and RRMSDs for the entirewhole and reduced grids, for the summer and winter study periods and for different depths.

Parameter	Considered grid		ROOI		DCT-PLS	
			Summer	Winter	Summer	Winter
<RMSD> (cm s^{-1})	Whole	U/V -12 m	3.79/5.08	4.46/6.28	3.59/3.62	3.10/2.65
		U/V -52 m	2.84/3.66	4.05/5.45	4.01/4.48	5.69/4.99
		U/V -100 m	2.69/3.14	3.89/5.31	4.10/3.22	8.45/5.32
	Reduced	U/V -12 m	6.35/3.87	8.29/3.91	4.15/2.77	3.92/1.93
		U/V -52 m	4.98/2.02	9.19/2.85	3.10/2.01	4.66/2.67
		U/V -100 m	4.31/1.77	8.38/2.46	2.33/1.75	3.66/2.59
<RRMSD>	Whole	U/V -12 m	0.83/0.83	0.84/0.88	0.88/0.64	0.67/0.38
		U/V -52 m	0.98/1.02	0.94/0.80	1.69/1.33	1.83/0.74
		U/V -100 m	1.05/1.04	0.92/0.80	1.82/1.07	2.79/0.83
	Reduced	U/V -12 m	0.56/0.94	0.53/1.04	0.37/0.74	0.25/0.53
		U/V -52 m	0.79/0.94	0.64/0.88	0.54/1.03	0.33/0.90
		U/V -100 m	0.95/1.04	0.72/0.80	0.54/1.00	0.32/0.95

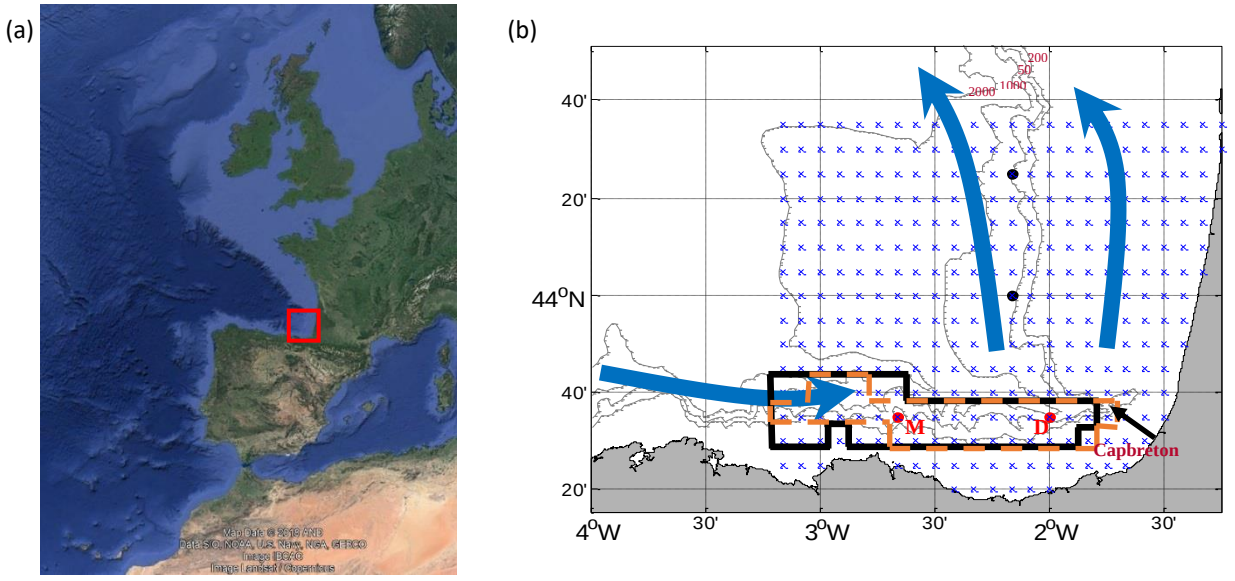

Figure 1. (a) Location of the study area (red square). (b) Close-up map of the study area. The winter IPC is represented by blue solid arrows. The grid used for the emulated HFR surface current fields is shown by blue crosses. The red dots provide the location of the current vertical profiles that emulate the EuskOOS moorings~~buoys~~: Matxitxako (red M) and Donostia (red D), whereas the black dots depict the location of the two extra moorings~~buoys~~ used for the 4-mooring~~buoy~~ scenario. The bold black lines delimit the winter reduced grid, whereas the dashed orange lines delimit the summer one. The grey lines show the 200, 500, 1000 and 2000 m isobaths.

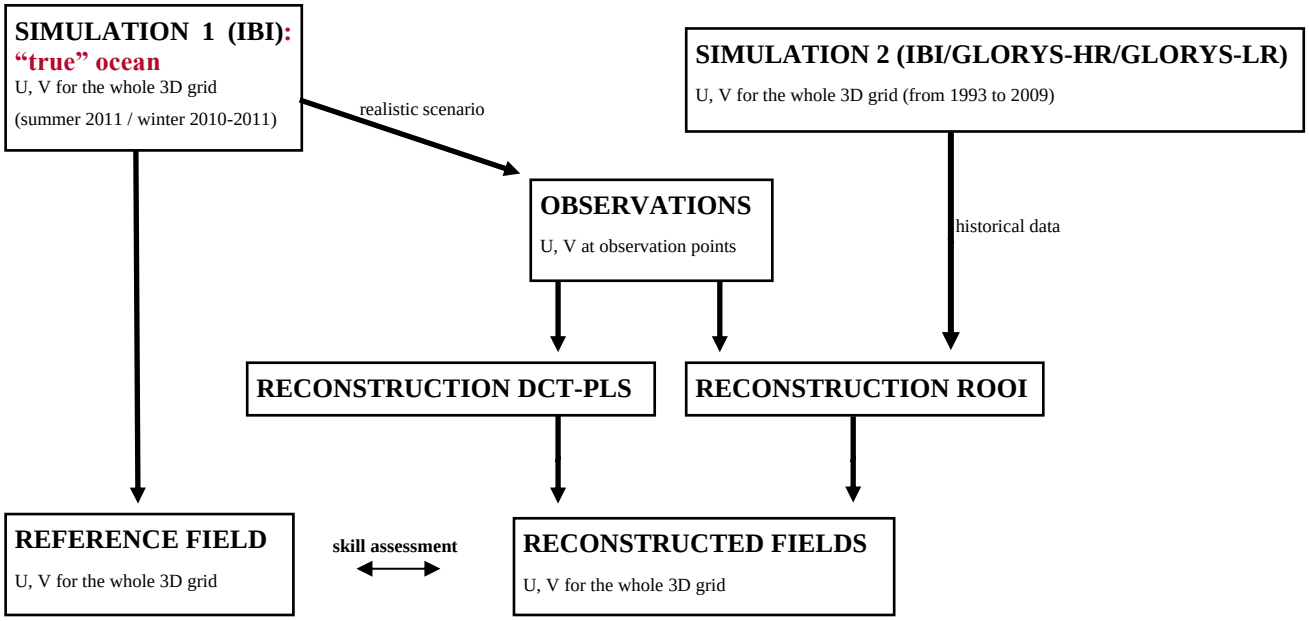

Figure 2. Scheme of the approach used to test the performance of the two data-reconstruction methods~~, that are~~ described in Sect. 2.2. The models used for SIMULATION 1 and SIMULATION 2 are presented in Sect. 2.3.

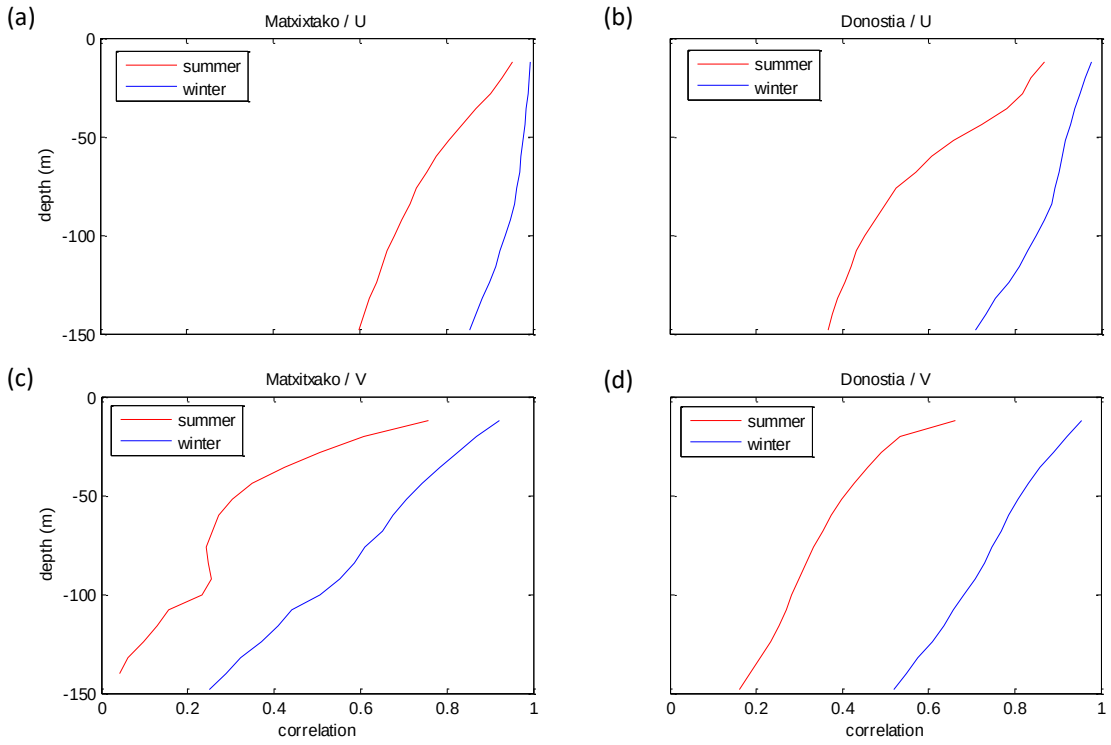

Figure 3. U (a, b) and V (c, d) temporal cross-correlation between the surface and the water column levels, for winter (blue) and summer (red) periods. In Matxitxako location (a, c) and in Donostia location (b, d).

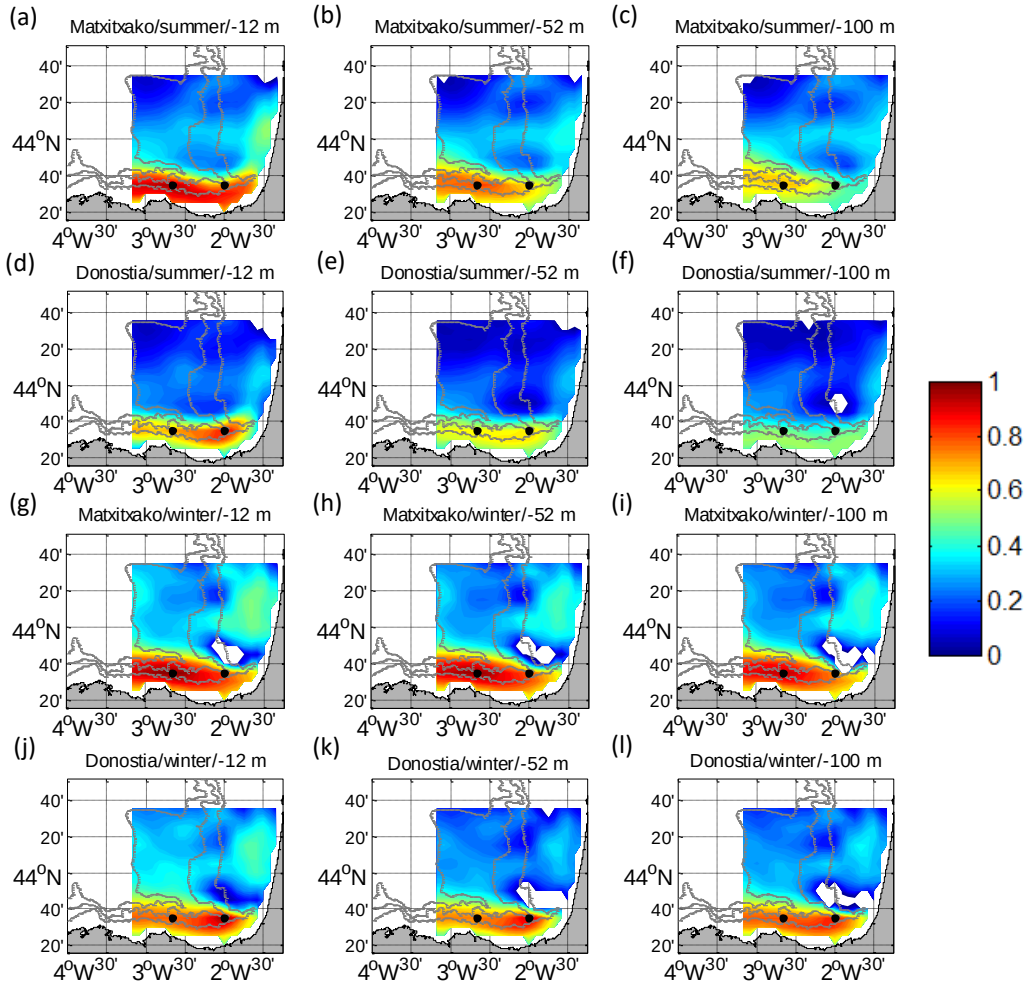

Figure 4. Temporal cross-correlation maps between the water column~~ADCP vertical~~ levels considered and the surface points of the HFR grid for U. a, b, c, g, h, i for Matxitxako mooring~~buoy~~ and d, e, f, j, k, l for Donostia mooring~~buoy~~. Different depths considered: -12 m (a, d, g, j), -52 m (b, e, h, k) and -100 m (c, f, i, l), for summer (a-f) and winter (g-l). The white gaps are the areas where the confidence level is less than 95%. The black dots depict the locations of the ~~ADCP~~current vertical profiles.

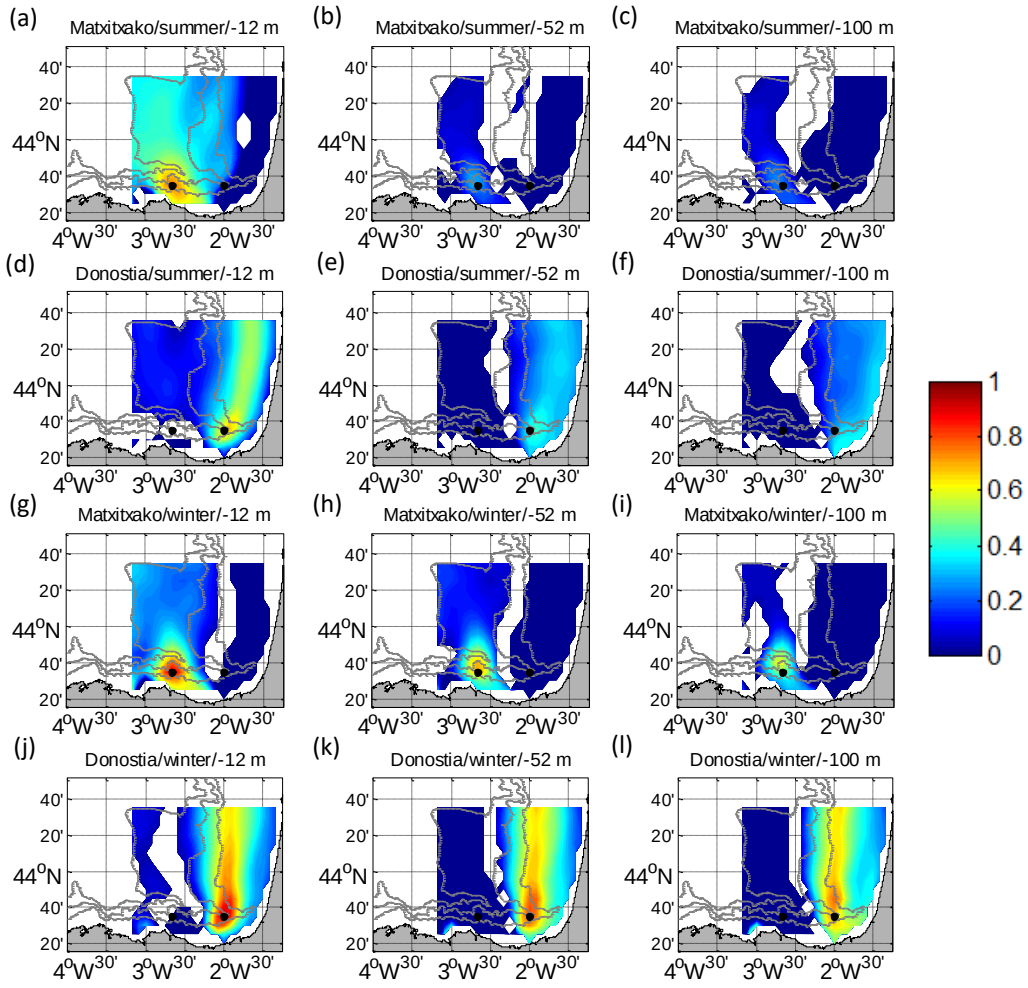

Figure 5. Temporal cross-correlation maps between the water column~~ADCP vertical~~ levels considered and the surface points of the HFR grid for V. a, b, c, g, h, i for Matxitxako mooring~~buoy~~ and d, e, f, j, k, l for Donostia mooring~~buoy~~. Different depths considered: -12 m (a, d, g, j), -52 m (b, e, h, k) and -100 m (c, f, i, l), for summer (a-f) and winter (g-l). The white gaps are the areas where the confidence level is less than 95%. The black dots depict the locations of the ~~ADCP~~current vertical profiles.

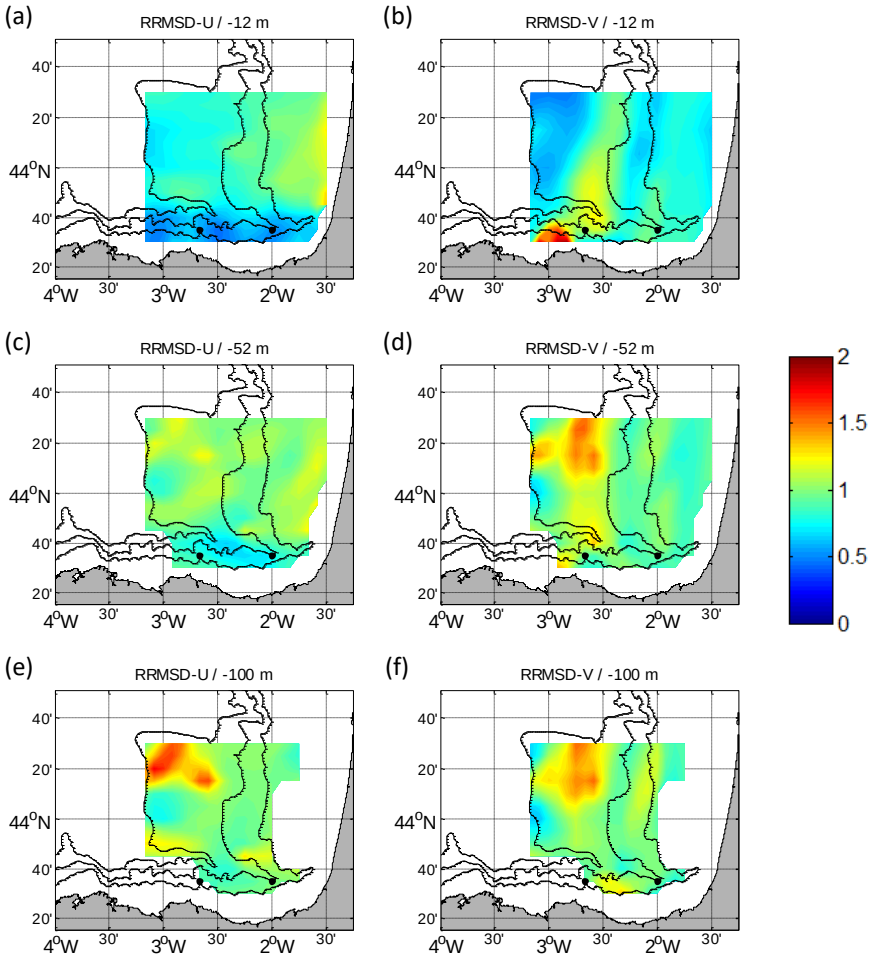

Figure 6. RRMSD maps for the summer period between the reference fields and the outputs of the ROOI with GLORYS-LR for U (a, c, e) and V (b, d, f). Different depths considered: -12 m (a, b), -52 m (c, d) and -100 m (e, f). The black dots depict the locations of the current vertical profiles~~ADCPs~~.

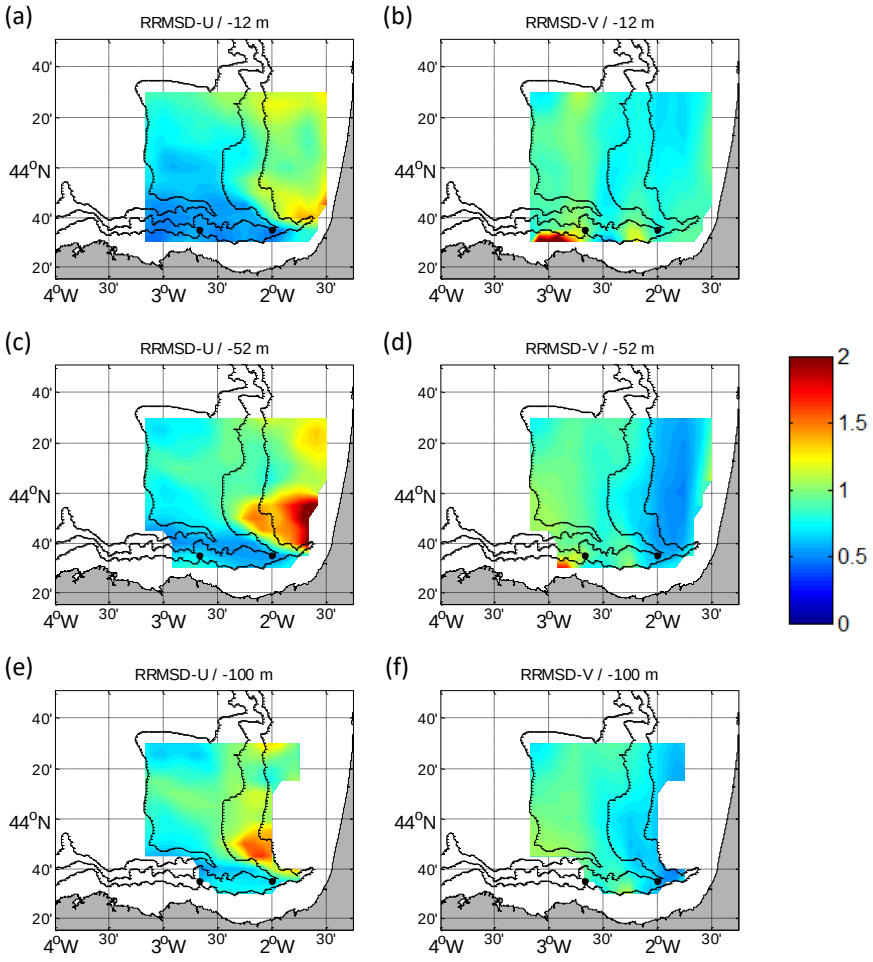

Figure 7. RRMSD maps for the winter period between the reference fields and the outputs of the ROOI with GLORYS-LR for U (a, c, e) and V (b, d, f). Different depths considered: -12 m (a, b), -52 m (c, d) and -100 m (e, f). The black dots depict the locations of the current vertical profiles~~ADCPs~~.

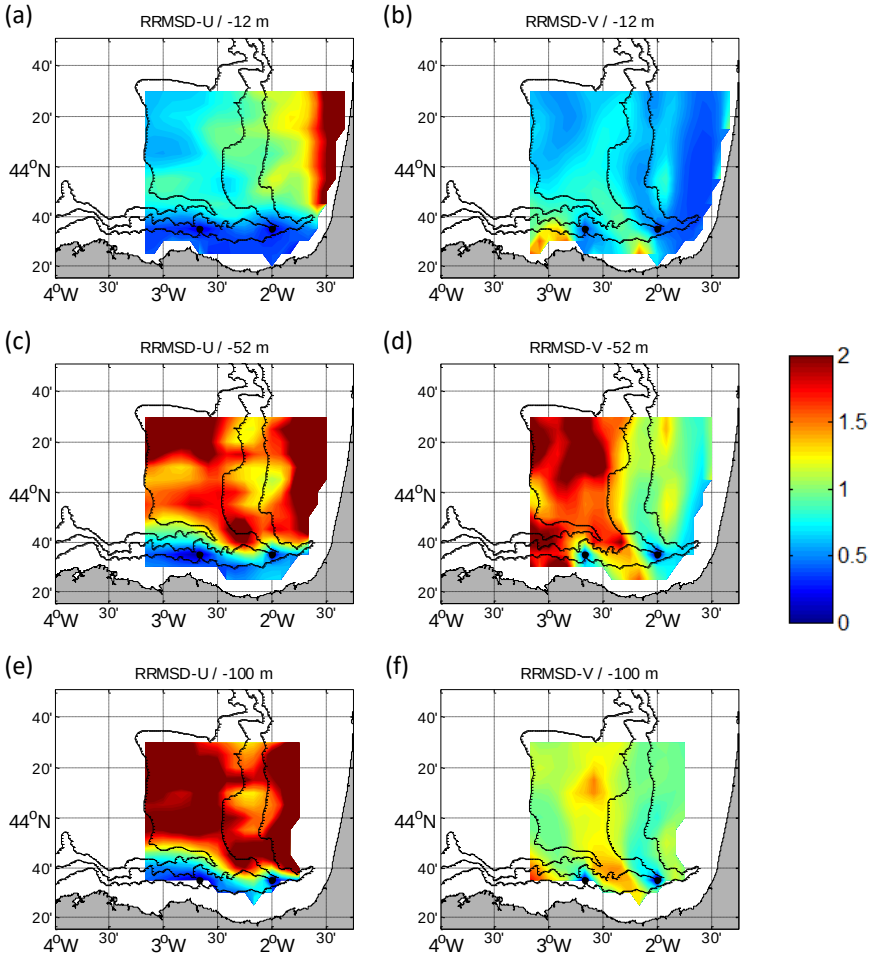

Figure 8. RRMSD maps for the summer period between the reference fields and the outputs of the DCT-PLS for U (a, c, e) and V (b, d, f). Different depths considered: -12 m (a, b), -52 m (c, d) and -100 m (e, f). The black dots depict the locations of the current vertical profiles~~ADCPs~~.

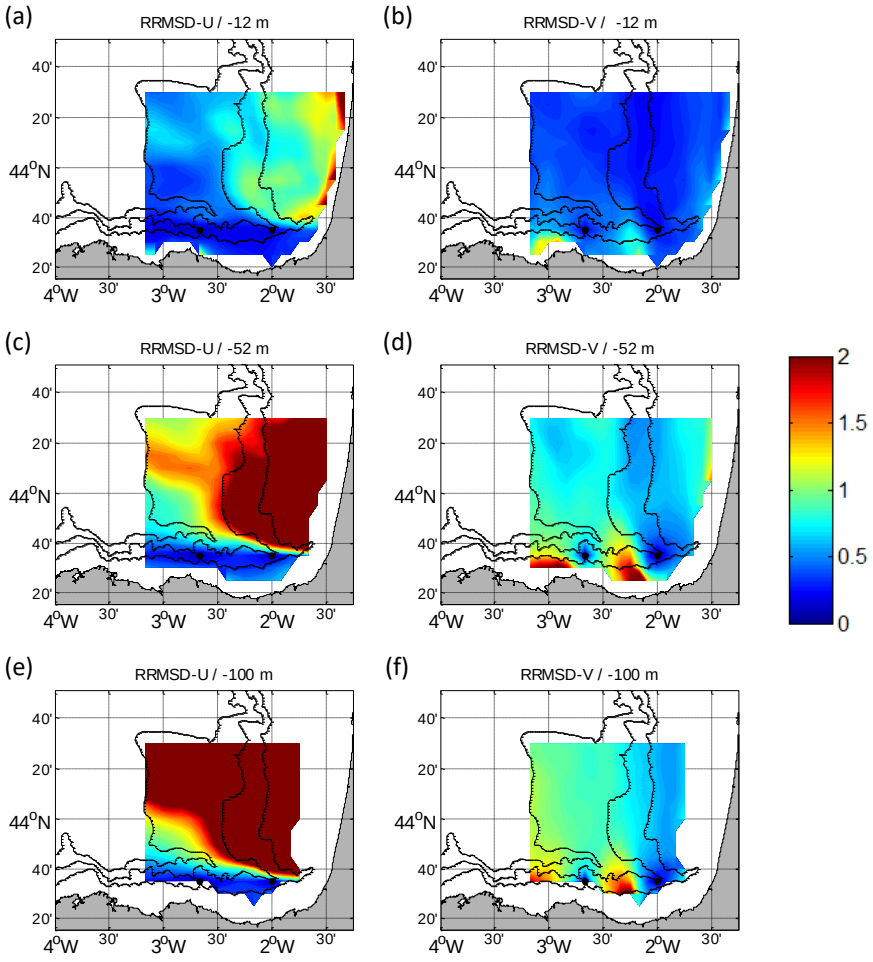

Figure 9. RRMSD maps for the winter period between the reference fields and the outputs of the DCT-PLS for U (a, c, e) and V (b, d, f). Different depths considered: -12 m (a, b), -52 m (c, d) and -100 m (e, f). The black dots depict the locations of the current vertical profiles~~ADCPs~~.

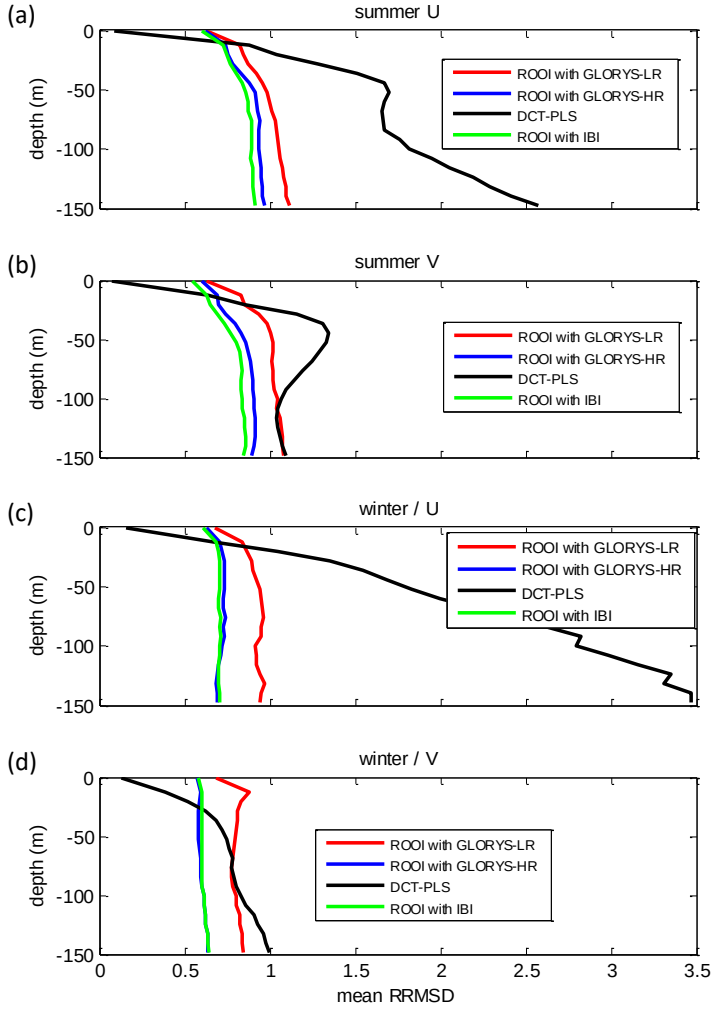

Figure 10. Mean RRMSDs related to all the data-reconstruction methods for each depth considering the entire~~whole~~ grid. For the summer period (a, b) and for the winter period (c, d). U in a, c and V in b, d.

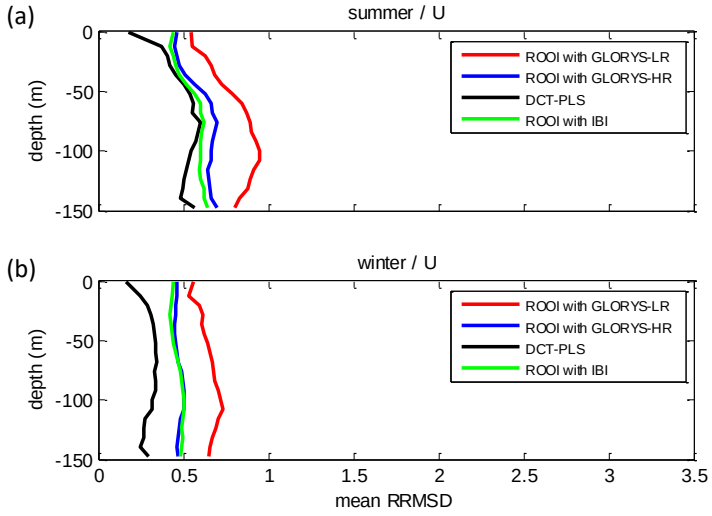

Figure 11. Mean RRMSD-U related to all the data-reconstruction methods for each depth considering the reduced grid domain. For the summer period (a) and for the winter period (b).

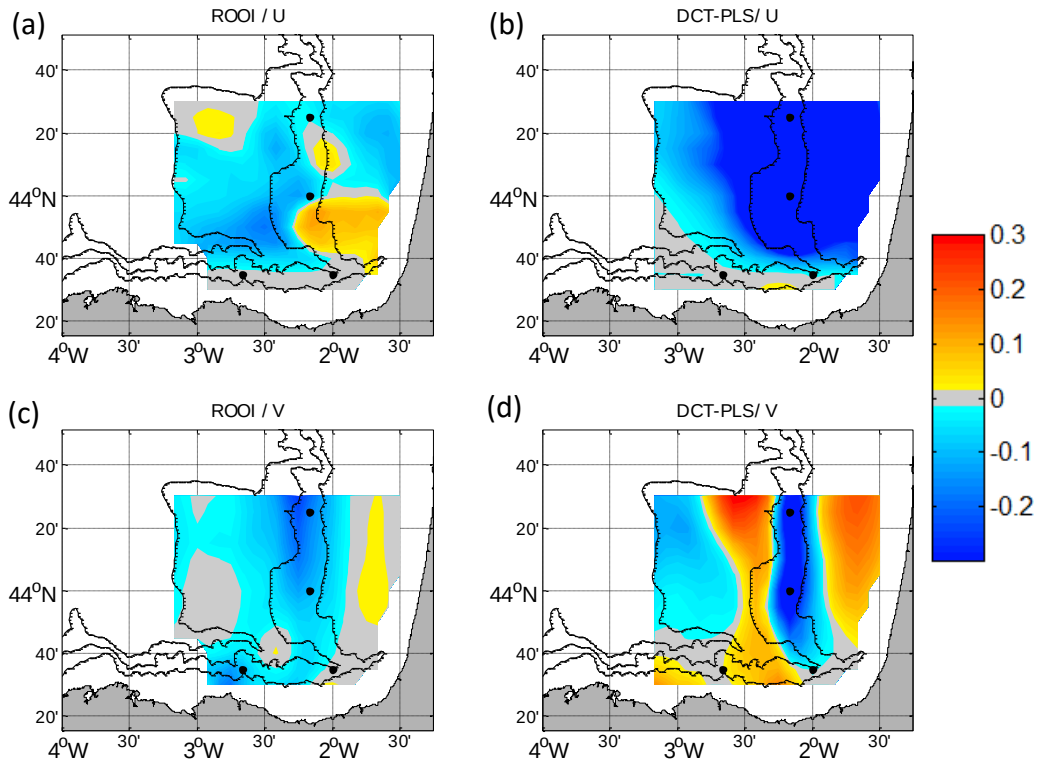

Figure 12. The 4-mooring~~buoy~~ scenario RRMSD maps subtracted by the 2-mooring~~buoy~~ scenario RRMSD maps for winter at -52 m. Negative~~, therefore, negative~~ values mean a better performance in~~with~~ the 4-mooring scenario for~~buoy configuration. For~~ U (a, b) and for V (c, d). For the ROOI (a, c) and for the DCT-PLS (b, d). The black dots depict the locations of current vertical profiles~~the ADCPs~~.

Supplementary Material

S1. Real HFR and ADCP observations data. Temporal cross-correlations with a confidence level of 99%. All the available data series of each dataset used. The results presented here complement the results shown in Rubio et al. (2019).

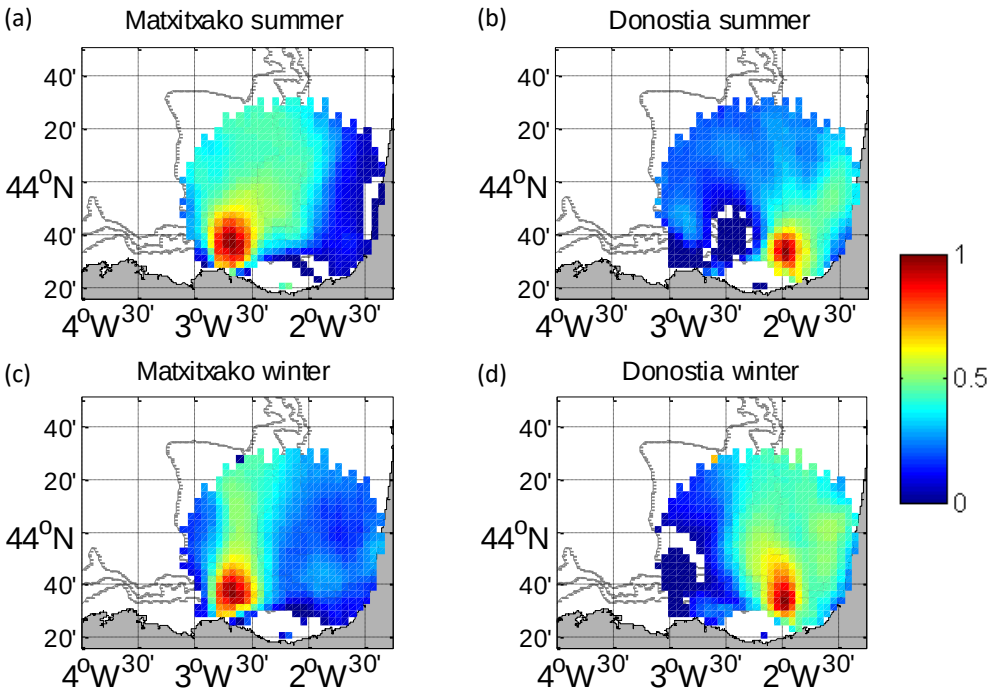

Figure S1. Temporal cross-correlation maps between the low-pass filtered time series of the HFR at Matxitxako (a, c) and Donostia (b, d) locations and the rest of the nodes within the HFR footprint area for V and for each season: summer (a, b) and winter (c, d). The results for the U component are shown in Rubio et al., 2019.

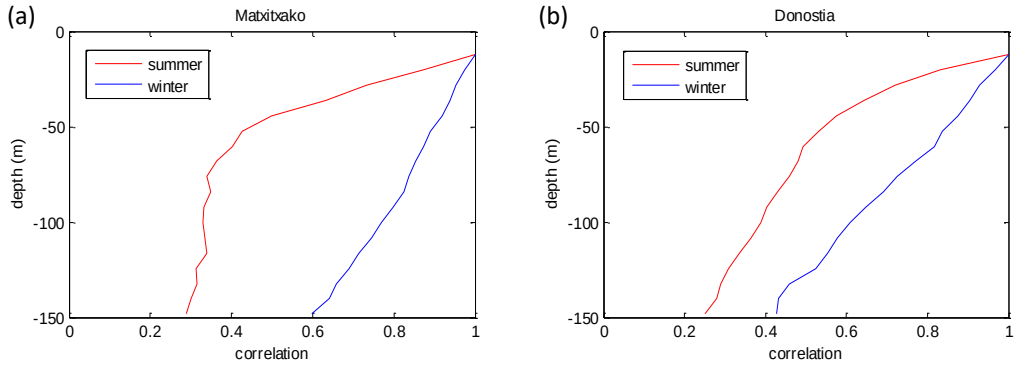

Figure S2. Low-pass filtered ADCP temporal V cross-correlations between the first bin (-12.26 m) and the rest of the bins along the water column for Matxitxako (a) and Donostia (b) for the summer (stratified) and winter (well-mixed) periods. The results for U are shown in Rubio et al., 2019.

5

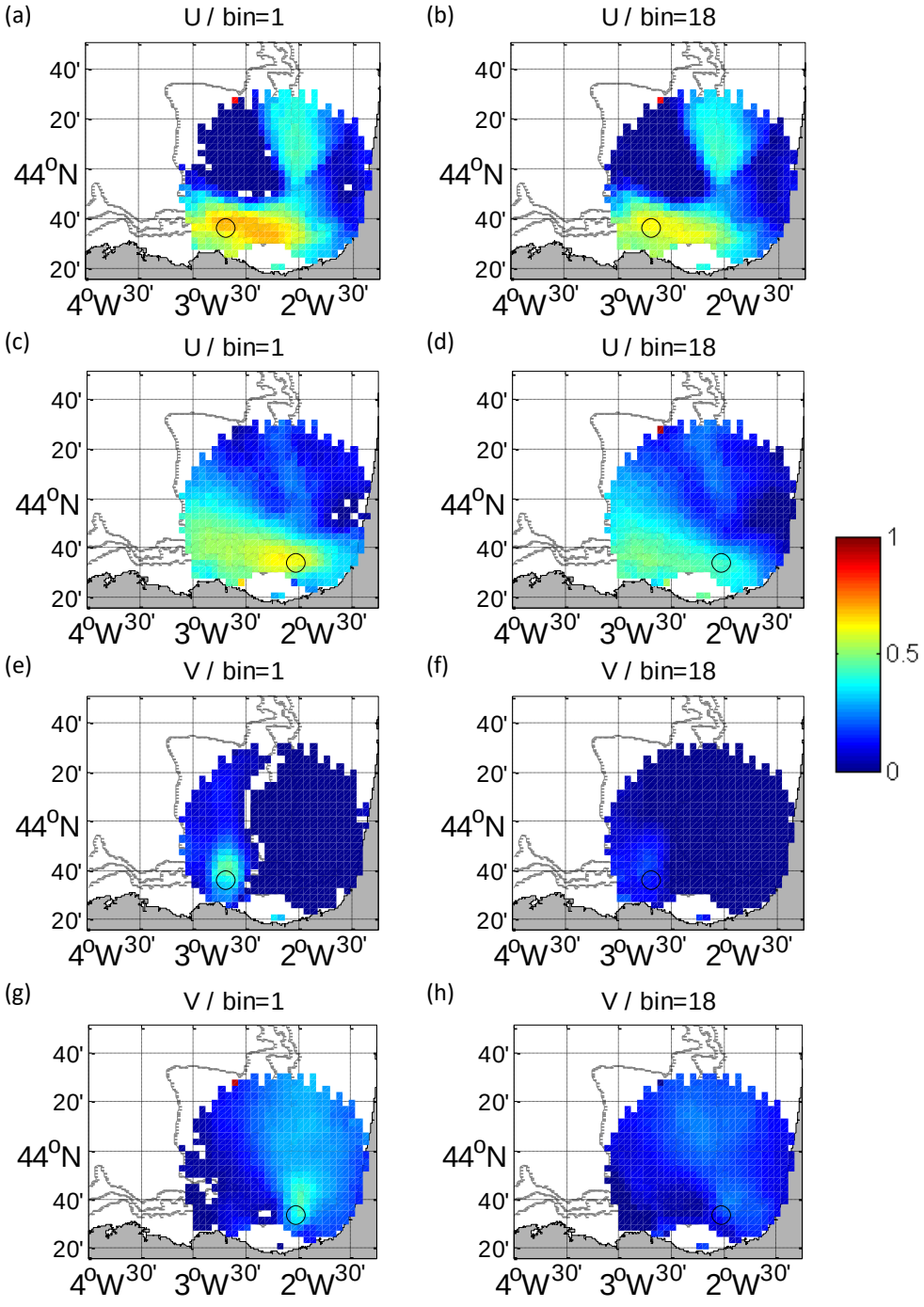

Figure S3. Temporal cross-correlation maps between the low-pass filtered time series of the HFR at the surface and the low-pass filtered ADCP time series for the bin 1 (-12.26m) (a, c, e, g) and 18 (-148.26m) (b, d, f, h) at Matxitxako (a, b, e, f) and at Donostia (c, d, g, h) and for U (a, b, c, d) and V (e, f, g, h). The black circles depict the positions of the ADCPs.

S2. RRMSD maps for ROOI with GLORYS-HR.

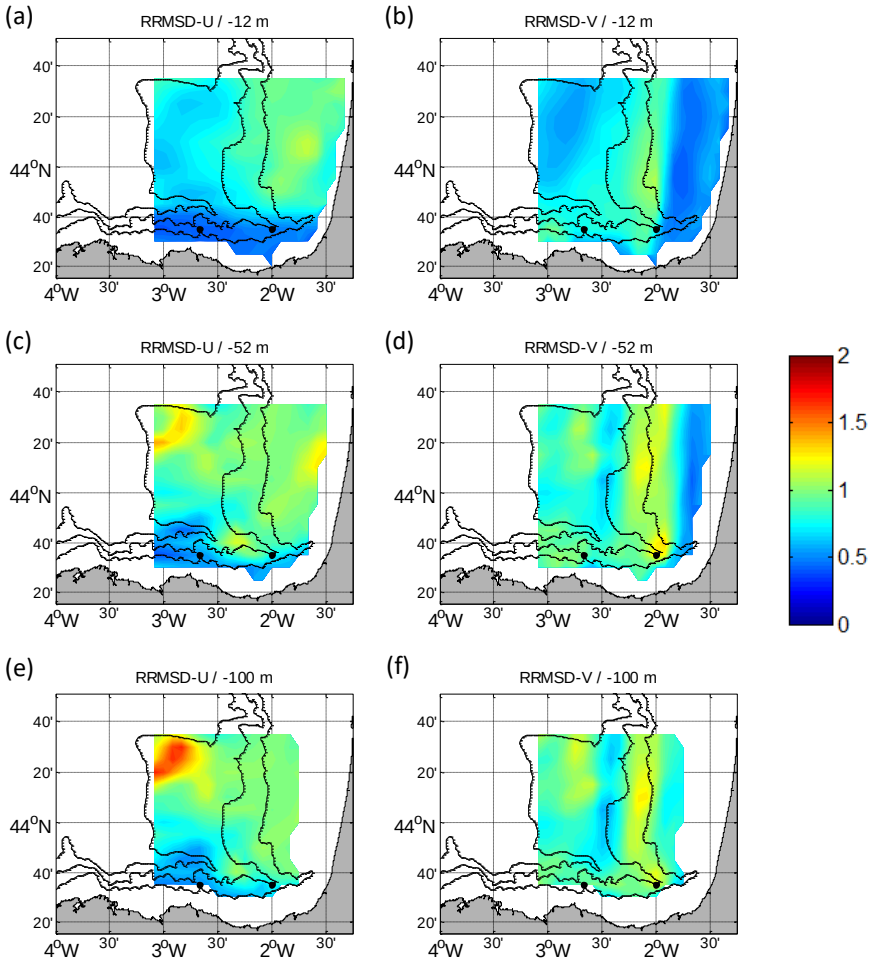

Figure S4. RRMSD maps for the summer period between the reference fields and the outputs of the ROOI with GLORYS-HR for U (a, c, e) and V (b, d, f). Different depths considered: -12 m (a, b), -52 m (c, d) and -100 m (e, f). The black dots depict the locations of the current vertical levels~~ADCPs~~.

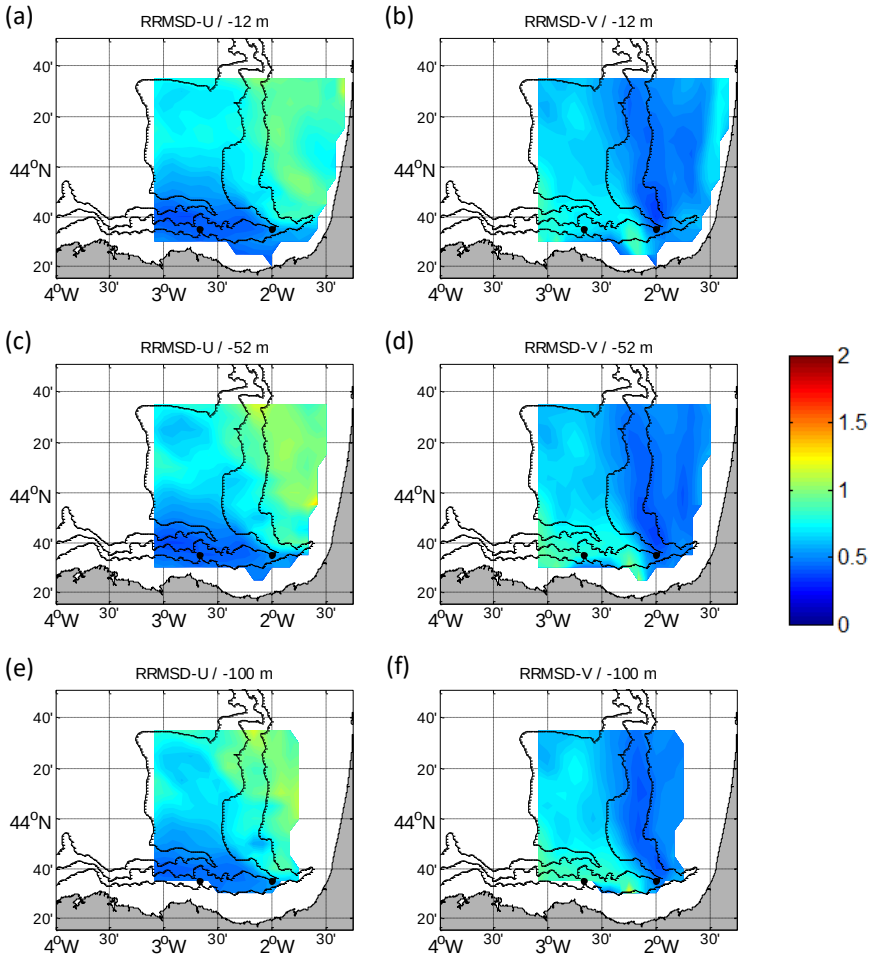

Figure S5. RRMSD maps for the winter period between the reference fields and the outputs of the ROOI with GLORYS-HR for U (a, c, e) and V (b, d, f). Different depths considered: -12 m (a, b), -52 m (c, d) and -100 m (e, f). The black dots depict the locations of the current vertical levels~~ADCPs~~.

S3. DCT-PLS RRMSD-U maps with higher colorbar values.

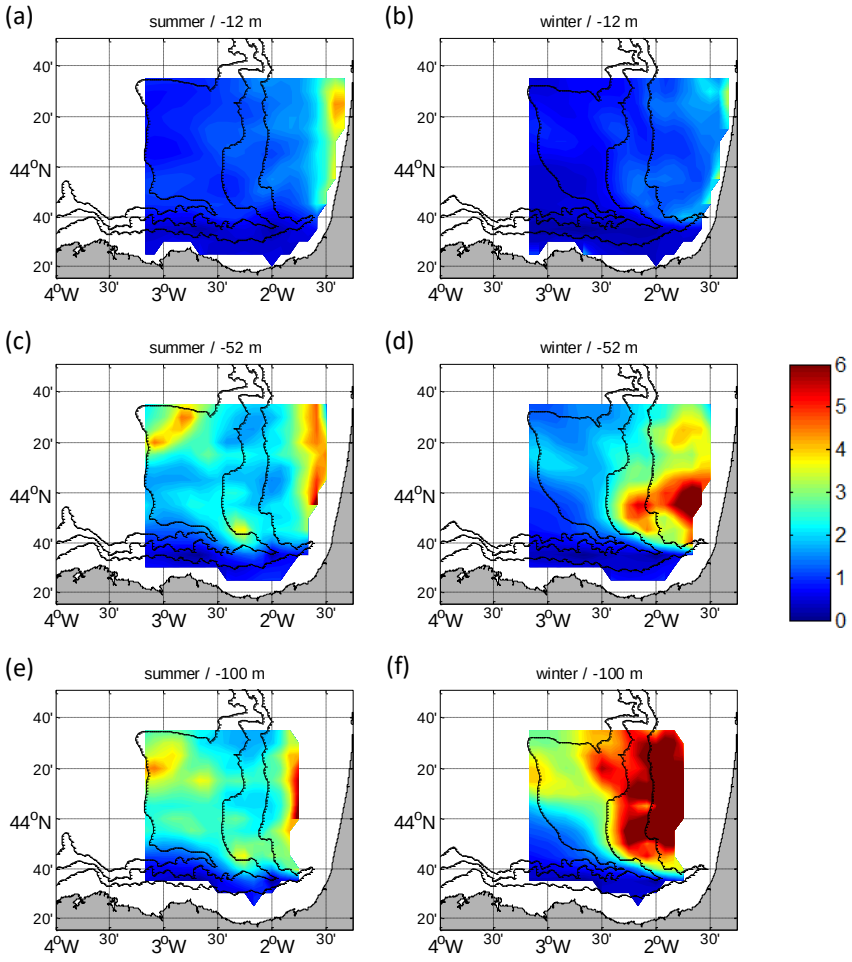

Figure S6. RRMSD-U maps for DCT-PLS for the summer period (a, c, e) and for the winter period (b, d, f).

S4. RMSD maps and spatial mean RMSD graphs.

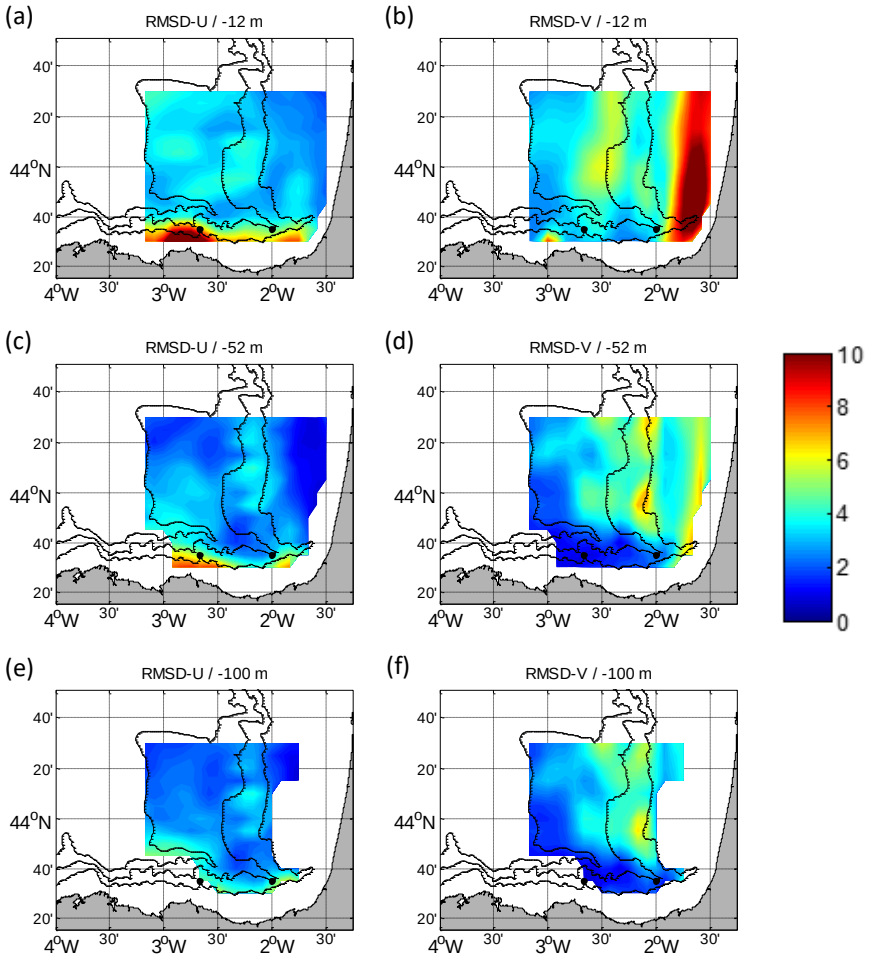

Figure S7. RMSD maps for the summer period between the reference fields and the outputs of the ROOI with GLORYS-LR for U (a, c, e) and V (b, d, f). Different depths considered: -12 m (a, b), -52 m (c, d) and -100 m (e, f). The black dots depict the locations of the current vertical profiles~~ADCPs~~.

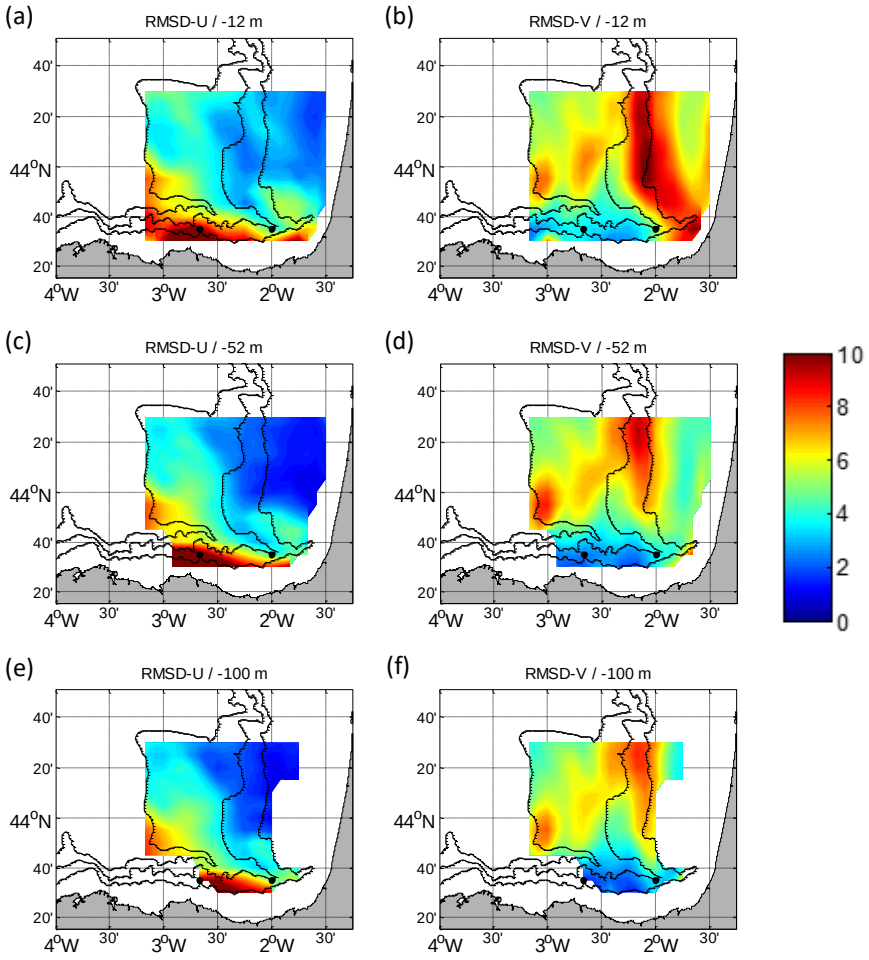

Figure S8. RMSD maps for the winter period between the reference fields and the outputs of the ROOI with GLORYS-LR for U (a, c, e) and V (b, d, f). Different depths considered: -12 m (a, b), -52 m (c, d) and -100 m (e, f). The black dots depict the locations of the current vertical profiles~~ADCPs~~.

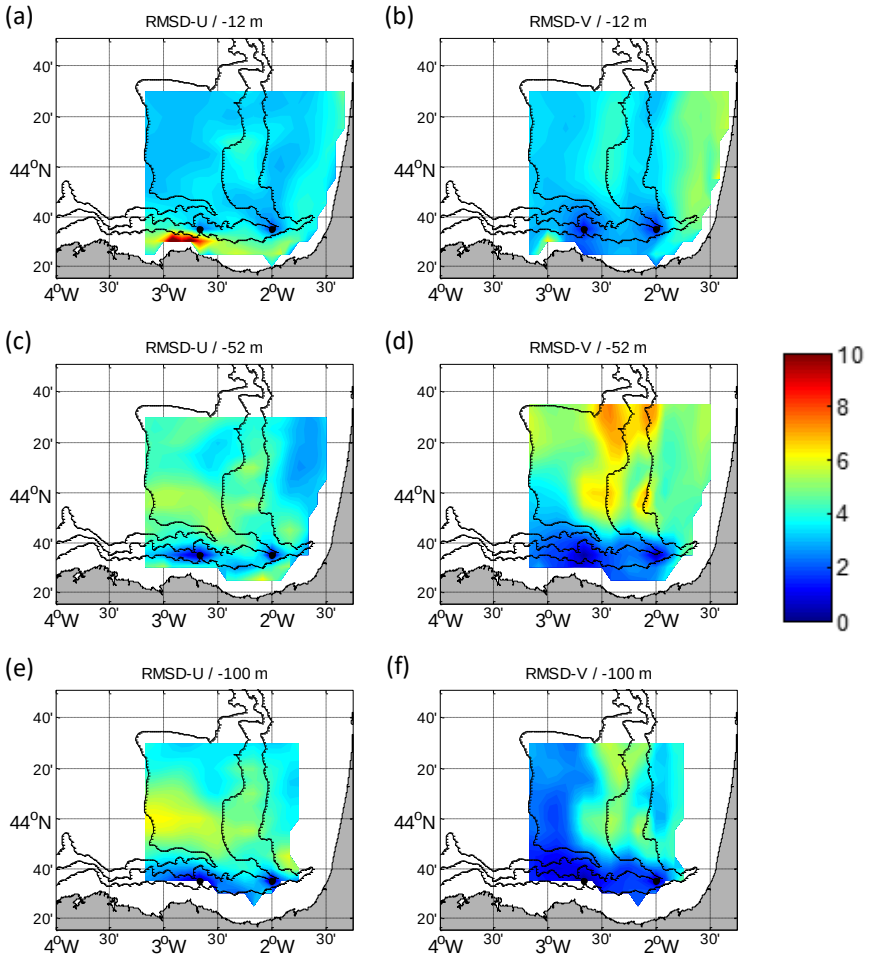

Figure S9. RMSD maps for the summer period between the reference fields and the outputs of the DCT-PLS for U (a, c, e) and V (b, d, f). Different depths considered: -12 m (a, b), -52 m (c, d) and -100 m (e, f). The black dots depict the locations of the current vertical profiles~~ADCPs~~.

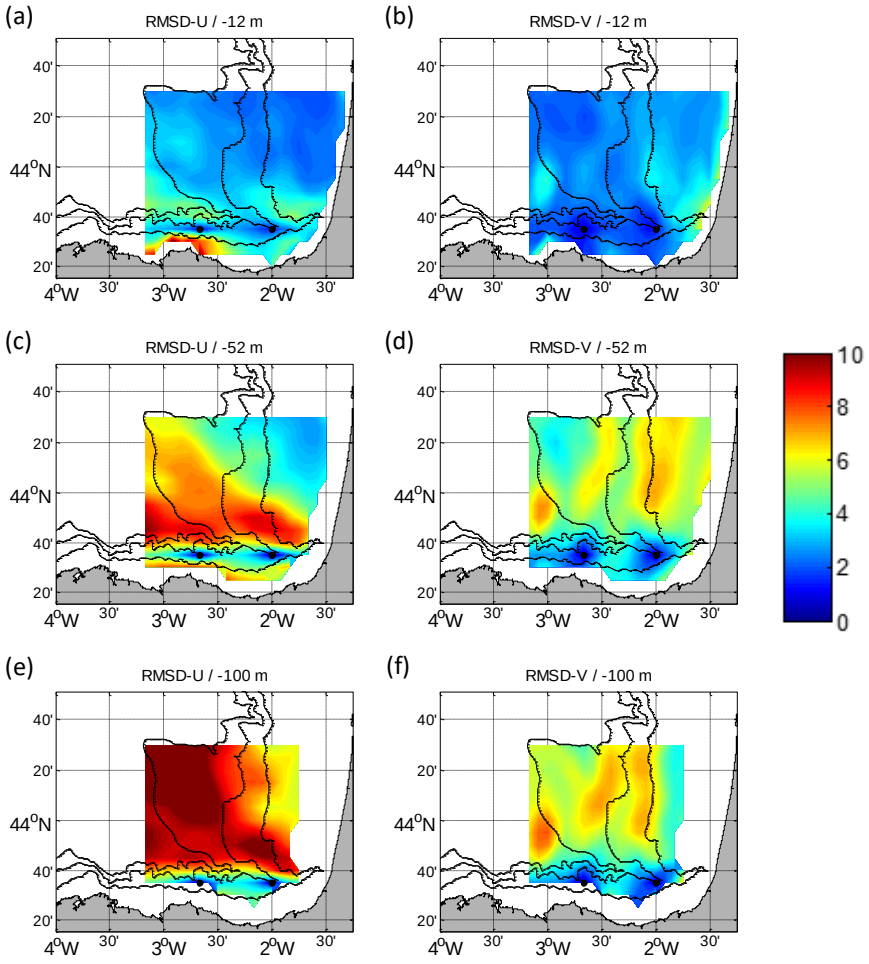

Figure S10. RMSD maps for the winter period between the reference fields and the outputs of the DCT-PLS for U (a, c, e) and V (b, d, f). Different depths considered: -12 m (a, b), -52 m (c, d) and -100 m (e, f). The black dots depict the locations of the current vertical profiles~~ADCPs~~.

5

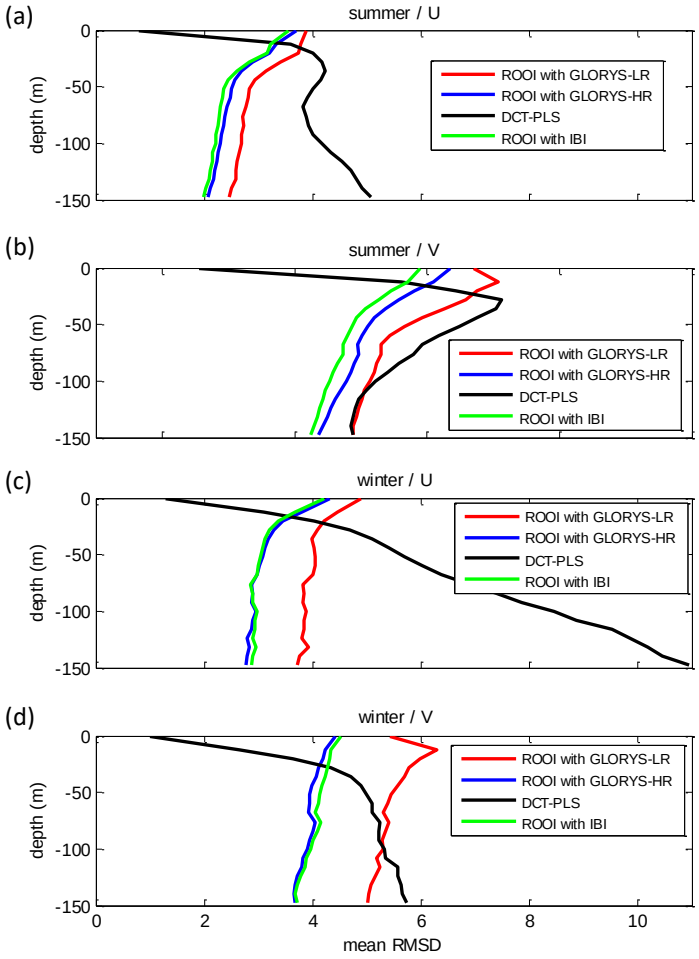

Figure S11. Mean RMSDs related to all the data-reconstruction methods for each depth considering the entire~~whole~~ grid. For the summer period (a, b) and for the winter period (c, d). U in a, c and V in b, d.

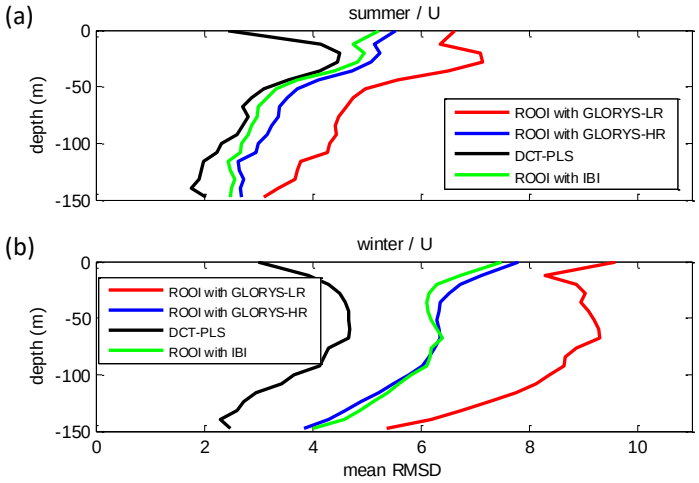

Figure S12. Mean RMSD-U related to all the data-reconstruction methods for each depth considering the reduced grid domain. For the summer period (a) and for the winter period (b).